Force Control

10

One of the fundamental requirements for the success of a robotic task is the ability of the control to handle the physical *interaction between robot and environment*. The quantity that more effectively describes the state of the physical interaction is the *contact force*. High values of contact force are generally undesirable since they can damage both the robot and the environment. In this chapter, the problem of controlling the physical interaction, modeled as an energy exchange between a mechanical *impedance* and a mechanical *admittance*, is first considered. The stability of the coupled system is guaranteed using the concept of *passivity*. Suitable *impedance control* and *admittance control* strategies are introduced, aimed at reshaping the dynamics of the robot based on the dynamics of the environment, modeled as a passive impedance or admittance. In the presence of geometric constraints imposed by the environment, the task geometry allows defining *natural constraints* set by the environment and *artificial constraints* set by the control; the constraints are referred to a suitable task frame. If the geometric constraints are available in analytic form, suitable selection matrices can be defined to separate the task directions where the robot is free to move from the constrained task directions. Hence, *hybrid force/motion control* schemes are derived, where motion and force are controlled along different task directions. This approach is also extended to manage the interaction with compliant environments. The case of redundant robots is finally presented.

10.1 The Force Control Problem

Robots are typically used to perform tasks that require pure motion and tasks that require *physical interaction*, exchanging forces with the environment. For example, in assembly lines of automotive factories, robot manipulators usually perform handling operations such as spray painting or glue deposition, which are pure motion tasks,

B. Siciliano et al., *Foundations of Robotics*, Advanced Textbooks in Control and Signal Processing, https://doi.org/10.1007/978-3-031-85523-8_10

but also tasks like surface polishing, removing material by carving or grinding, and assembling mechanical parts, during which physical interaction with the environment occurs through a specialized tool or a gripper as the end-effector.

Many service robots are designed to work in close proximity with humans, or for direct human–robot interaction, also physical, within a shared space. These kinds of robots, known as collaborative robots or *cobots*, are also being used in industrial applications to perform unergonomic tasks such as helping workers move heavy parts, or feeding machines, or assembly.

To ensure safety during physical interaction, a fundamental requirement is *compliance*. Compliance allows keeping the forces exchanged during the interaction limited and can be achieved both in a passive and in an active way.

Passive compliance[1] can be obtained by using soft materials and flexible mechanical interfaces. An example of a device with passive compliance for industrial assembly operations is the so-called remote center of compliance (RCC) (see Fig. 10.10 in Sect. 10.2.4), which allows achieving a selective compliant behavior, e.g., different but fixed compliance along or about different directions, so that assembly is facilitated by small accommodation of the workpiece carried by the manipulator. Robots intended for physical human–robot interaction may include flexible actuation/transmission elements to enhance safety (see Chap. 11).

The alternative to passive compliance is to actively achieve selective compliant behavior, using control. *Active compliance* allows the setting and modifying of compliance by software, according to the task requirements. *Force control* refers to control approaches that allow the robot to achieve active compliance or, more generally, are designed to be effective in the case of physical interaction of the robot with the environment.

Force control strategies are employed in many robotic fields, such as grasping, cooperative robotics, telemanipulation, locomotion, just to mention a few. Many but not all force control approaches make use of the feedback of the interaction force measured through suitable force sensors.

A typical force sensor for industrial applications is the *wrist force/torque sensor*, mounted on the basis of the end-effector, which allows the measurement of the three components of a force and the three components of a moment with respect to a frame attached to the end-effector itself (see also Sects. 1.4.2 and 3.10.3).

Contact forces can also be estimated by using torque sensors in the robot joints, if available, or using the measurements of the currents of the joint actuators, which are proportional to the torques (see also Sects. 1.4.1 and 6.2.1). Joint torque sensors are especially useful if the interaction occurs not at the end-effector but on the robot body, and for this reason they are often present in cobots.

[1] The term ‘passive compliance’ is used here, in antithesis to ‘active compliance’, to denote compliance not achieved by control. It is not related to the concept of passivity and passive system in the energetic sense, as defined in Appendix D and also used in this chapter.

Other force sensors can be placed on robotic fingers and are generally tactile, in the sense that they allow measuring both the *contact force* and locating the area of contact. These sensors can be used for grasp control, as discussed in Chap. 12.

To fully analyze the physical interaction of a robot with a surface, an object or a human[2] there are three different situations to be considered:

- free motion, when the robot is not in contact with the environment;
- transition from free motion to contact and vice versa;
- the robot and the environment are in contact.

The problem of controlling the robot before contact, or after that contact is lost, is a motion control problem, but it is closely related to force control during the transition phases, when the robot is making or breaking contact. The control of transitions is very challenging and is not considered here. In the following analysis, it is assumed that the robot is already in contact with the environment and that the contact is not lost during task execution.

10.1.1 Control of Robot Physical Interaction

During physical interaction, which may occur through a contact point or a distributed surface, there is an exchange of mechanical power between the robot and the environment. This power can be computed as the scalar product of a velocity $\boldsymbol{v}$ and a force $\boldsymbol{f}$ defining an *interaction port*, as follows:

$$\mathcal{P} = \boldsymbol{f}^T \boldsymbol{v}. \tag{10.1}$$

With a slight abuse of notation, vector $\boldsymbol{v}$, representing the common velocity of the robot and of the environment at the interaction port, can be either a twist $\boldsymbol{t}$ or is the time derivative $\dot{\boldsymbol{y}}$ of a task vector $\boldsymbol{y}$; correspondingly, vector $\boldsymbol{f}$, representing the force applied to the robot by the environment, is a wrench $\boldsymbol{w}$ or a vector $\boldsymbol{\gamma}$ of generalized forces performing work on the task variables. According to Newton's third law of action and reaction, the force applied to the environment by the robot is $-\boldsymbol{f}$. Hence, in order to have a controlled physical interaction, the two quantities that can be controlled are the velocity $\boldsymbol{v}$ and the force $\boldsymbol{f}$ at the interaction port.

Using physical intuition, it is clear that it is not possible to control velocity and force at the same time because if one system (the controlled robot) imposes velocity, the corresponding force depends on the velocity itself and on the dynamics of the other system (the environment) and vice versa. Therefore, three options are available for a controlled physical interaction:

- controlling the velocity (or the position) of the robot;

[2] Hereafter, the two interacting systems are referred as *robot* and *environment*.

- controlling the force exerted by the robot on the environment;
- controlling the dynamic relationship between force and velocity.

The last option is known as *impedance control*. Selecting the most suitable control strategy is often not easy and depends on the particular task, but also on the kind of robot and on the dynamics of the environment. Some examples are given below.

When the robot interacts with an *inertial* environment (e.g., a robot manipulator lifting an object), it makes more sense to control the velocity (or position) of the robot because it is more important to follow a given path in a given time rather than imposing a given force on the object. In this case, the inertial contribution to the interaction force can be reasonably kept limited by limiting the acceleration imposed on the object (the gravity contribution cannot be modified, of course). For the design of the motion controller, the interaction force can be considered as an external disturbance, or a parametric uncertainty, or else taken into account in the robot dynamics.

Similarly, if the interaction force is of *damping* type (viscous friction or damping proportional to the velocity, e.g., in the case of a mobile robot pushing a box with negligible inertia sliding on the floor), the force can be kept limited by reducing the controlled velocity.

On the other hand, when the environment is of *elastic* type (i.e., it behaves like a spring which returns to its original shape when the forces causing the deformation are removed), or when the elasticity is the dominant property of the physical behavior of the environment, it is still possible to control the robot velocity (or position). In fact, if the robot presses against an elastic-type deformable surface with a constant stiffness coefficient, the interaction force is proportional to the deformation. However, a pure motion control strategy may fail, especially when the stiffness coefficient is high. In fact, uncertainty in the knowledge of the stiffness coefficient and on the position of the surface may produce large forces when the motion controlled robot attempts to reach a desired position that corresponds to a large deformation. The force may overcome the threshold that produces damages in the interacting parts or saturation of the robot actuators—stability is at risk! In this case, a control strategy aimed at imposing a given force and not a given motion (velocity, position) is more appropriate.

In view of the examples considered, we can conclude the following.

- Pure *motion control* is suitable to manage the interaction with environments of inertial or damping type or, as a limit case, if no interaction occurs, when the force (as well as the exchanged mechanical power) is null for any velocity.
- Pure *force control* is suitable in the presence of high interaction forces in response to relatively small robot displacements; that is, when the environment is of elastic type and the stiffness coefficient is high. The limit case is when the environment is rigid (infinite stiffness); in this case, along the directions where interaction occurs, the velocity (as well as the exchanged mechanical power) is always null and the contact force can be arbitrarily imposed.
- In intermediate situations, a possible alternative is to use *impedance control*, which is not intended to impose on the robot a given motion or an interaction force, but

rather to achieve for the controlled robot a desired dynamic behavior between velocity (or position) and force at the interaction port.

It is important to note that a real situation of physical interaction is often a distributed phenomenon in which the local geometric and physical characteristics of the contact surfaces as well as the global dynamics of the robot and of the environment are involved. Moreover, there are tasks where the environment imposes geometric constraints on the end-effector motion. In these situations, the interaction forces include constraint forces, i.e., reaction forces that arise when the end-effector tends to violate the constraints. This happens, for example, in the case of a robot sliding a rigid tool on a rigid surface or a robot turning a crank.

An accurate mathematical model that allows capturing all these phenomena is often difficult to obtain. Therefore, interaction control laws are usually designed on the basis of simplifying assumptions. The effectiveness in real situations, where some of the ideal assumptions are relaxed, is entrusted to the robustness of the feedback control.

Different categorizations of force control laws exist. In this chapter, two main control approaches are illustrated. The first is based on *impedance control*, which is usually adopted when the environment model is not available or uncertain, and the interaction is modeled as an exchange of mechanical power between passive systems, i.e., systems that cannot generate energy. The second is based on *hybrid force/motion control*, which is useful especially in the presence of geometric constraints and consists in controlling the motion along the unconstrained task directions and the force along the constrained task directions.

10.2 Impedance Control

Impedance control is based on the concepts of mechanical *impedance* and *admittance* at an interaction port, which are analogous to the electrical impedance and admittance of a bipolar circuit. The power flowing through a port is the product of an effort variable and a flow variable. In the mechanical domain, the effort variable is the force (analogous to a voltage) and the flow variable is the velocity (analogous to a current).

10.2.1 Impedance and Admittance

A mechanical impedance at an interaction port can be defined as the dynamic operator that determines an output force in response to an input velocity at the same port.

A mechanical admittance at an interaction port can be defined as the dynamic operator that determines an output velocity in response to an input force at the same port.

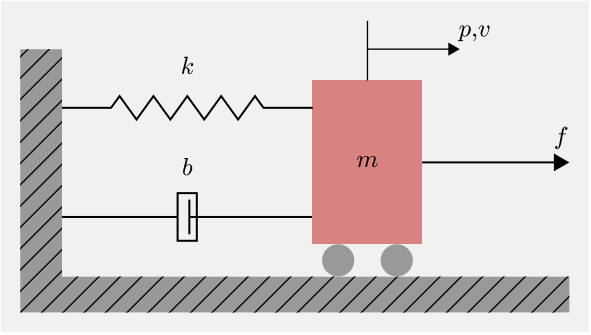

Fig. 10.1 Mass–spring–damper system

In the linear scalar case, impedance and admittance can be represented as transfer functions in the Laplace domain, denoted as $Z(s)$ and $Y(s)$ respectively, and the corresponding transfer functions are reciprocal, i.e, $Z(s) = 1/Y(s)$.

A typical example of linear mechanical impedance and admittance is presented in the following.

Example 10.1 Consider a mass m attached to a spring of stiffness k, in the presence of viscous friction represented by the damper b, which translates along a single direction subject to an interaction force f (see Fig. 10.1). The equation of motion can be written in the form

$$f = m\dot{v} + bv + kp,$$

where the position p is the integral of the velocity:

$$p(t) = \int_0^t v(\tau)d\tau.$$

In the Laplace domain it is easy to compute the output velocity $v(s)$ from the input force $f(s)$ in the form

$$v(s) = \frac{1}{ms + b + \dfrac{k}{s}} f(s) = Y(s)f(s),$$

where

$$Y(s) = \frac{s}{ms^2 + bs + k}$$

is the mechanical admittance of the system. The impedance can be computed as $Z(s) = 1/Y(s)$.

Note that in this example, the admittance $Y(s)$ is a (strictly) proper transfer function. This means that it is realizable, i.e., it can be described by a standard finite-dimensional linear state-space equation. On the other hand, the impedance $Z(s)$ is not proper and thus not realizable. ■

In a more general situation, the mechanical impedance equation can be multivariable and nonlinear. In the latter case, the Laplace transform cannot be used, and there is no general formulation of the impedance and admittance equations. The EL equations of a robotic system can be easily rewritten into a state equation and an output equation as:

$$\dot{\boldsymbol{x}}(t) = \boldsymbol{g}_Y(\boldsymbol{x}(t), \boldsymbol{f}(t)) \tag{10.2}$$

$$\boldsymbol{v}(t) = \boldsymbol{h}_Y(\boldsymbol{x}(t), \boldsymbol{f}(t)) \tag{10.3}$$

defining a nonlinear admittance. In the above equations, $\boldsymbol{x}(t) \in I\!R^n$ is the internal state of the system, $\boldsymbol{f}(t) \in I\!R^m$ is the vector of the nonconservative forces acting on the system, taken as input, $\boldsymbol{v}(t) \in I\!R^m$ is the output velocity and $\boldsymbol{g}_Y$, $\boldsymbol{h}_Y$ are, in general, nonlinear functions. The corresponding impedance can be found by inverting *causality*, that is, by exchanging the role of the input and output. However, as for the linear case, the resulting input–output relationship does not have the above standard form. For instance, the joint-space dynamic model (5.39) of a robot moving in free space can be easily put in nonlinear admittance form with state vector $\boldsymbol{x} = (\boldsymbol{q}, \dot{\boldsymbol{q}})$, input force $\boldsymbol{\tau}$ and output velocity $\dot{\boldsymbol{q}}$. Vice versa, if the velocity $\dot{\boldsymbol{q}}$ is taken as input and the torque $\boldsymbol{\tau}$ is taken as output, then the impedance is the input–output relationship resulting from the solution of an inverse dynamics problem (see Sect. 5.1). This is the nonlinear counterpart of the improper impedance transfer function for the simple mechanical system considered in Example 10.1.

The physical interaction of the controlled robot with the environment can be modeled as an exchange of mechanical power at an interaction port of two physical systems modeled as impedance or admittance. In principle, the controlled robot and the environment, taken separately, could be represented both as impedance and admittance. However, when they interact, the causality of the robot and of the environment must be reciprocal, because the output of one system must be the input of the other and vice versa. The appropriate causality of each system often depends on the features of the environment and of the robot, as well as on the task.

For instance, if the environment is a rigid surface, the velocity along the direction orthogonal to the surface is constrained to be zero (geometric constraint), and thus it cannot be imposed. This implies that the input variable of the environment at the interaction port must be the force and the environment must be modeled as an admittance, which is zero in the direction orthogonal to the surface. On the other hand, if the robot is driven by actuators that use transmissions with poor backdrivability (see Sect. 1.3.2), then it is more convenient to model the robot as an admittance which imposes a velocity to the environment.

Figure 10.2 shows one of the two possible causal interconnections between the robot and the environment, where the robot is modeled as an impedance, and the environment is modeled as an admittance. Note that, at the interaction port, the velocities of the two systems are the same ($\boldsymbol{v}_{\text{env}} = \boldsymbol{v}$), whereas the forces acting on the systems have opposite signs ($\boldsymbol{f}_{\text{env}} = -\boldsymbol{f}$), according to Newton's third law of action and reaction.

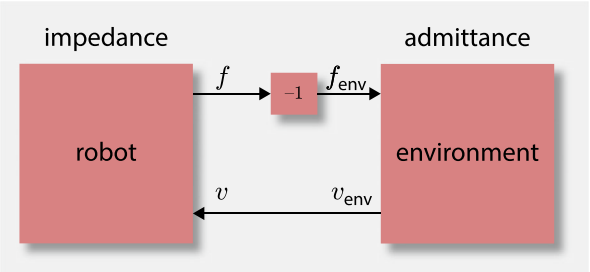

Fig. 10.2 Connected impedance/admittance with common velocities and opposite forces at the interaction port

It is important to recognize that the velocity $\boldsymbol{v}$ and the force $\boldsymbol{f}$ at the interaction port depend on the dynamics of both the robot and the environment and cannot be predicted in the absence of complete characterization of both systems. On the other hand, the impedance or the admittance are independent of each other. Therefore, the impedance or admittance of the robot can be modified by using feedback control, regardless of the environment. The impedance (admittance) of a controlled robot at the interaction port is usually denoted as *apparent* impedance (admittance).

10.2.2 Coupled Stability

The idea of impedance control is that of designing a feedback control law that allows the robot to behave like a desired impedance or a desired admittance at the interaction port.

According to this view, a successful controller does not have the objective of ensuring tracking or regulation of one or more physical variables of the system but of satisfying the following goals:

- coupled stability regardless of the environment, or for certain class of environments;
- satisfactory performance, in terms of minimal deviation of the apparent impedance (or admittance) from the desired one.

Coupled stability here means at least marginal stability during the interaction. The above goals guarantee good behavior during the transient and at steady state, for both force and velocity, if the desired impedance or admittance is well selected.

Concerning stability, it is important to note that a system that is stable in isolation can become unstable when coupled to another system that is itself stable. Therefore, the issue of coupled stability is of the utmost importance.

The concept of stability of systems that exchange power at an interaction port can be related to that of *passivity*. Passivity quantifies the notion that the energy that a system can deliver, for any time period, at its port of interaction cannot be greater than the energy that, in total, is input into the system from the same port for all time. A passive system cannot generate energy, and the power injected into the system

can only be dissipated or stored. The definitions of passive systems and their main properties, both for linear and nonlinear systems, are summarized in Appendix D.3.

In the single-input single-output linear case, a 1-port linear impedance Z is *passive* if the transfer function $Z(s)$ is positive real (PR). The same property holds for a 1-port linear admittance Y.

The dynamic system composed of the controlled robot and the environment interacting via their respective power variable pairs can be decomposed as a negative feedback interconnection of an impedance and an admittance. The coupled stability can be analyzed using results of passivity theory (see Appendix D.3). In particular, the negative feedback interconnection of two passive systems is still passive and stable; moreover, if one of the two systems satisfies additional conditions (e.g., strict passivity), then asymptotic stability is ensured.

In view of the above considerations, it can be inferred that if a robot is controlled so that it behaves like a passive impedance or admittance at the interaction port, then coupled stability is ensured for any passive environment.

This is an important result of practical application in interaction control, although there are some limitations.

- The passivity of the controlled robot and of the environment is only a sufficient condition for coupled stability, also in the linear case; even though one of both systems are not passive, the coupled system can be stable or asymptotically stable.
- Passivity is very useful to guarantee stability when the model of the environment is not available or uncertain (and this is a very frequent situation); however, it is often too conservative and it produces poor transient performance, so that, in some situations, it is intentionally violated.
- Although stability is guaranteed for any passive environment, the transient behavior of the coupled system depends on the actual dynamics of the environment and of the robot. Hence, a model of the environment is required for parameter tuning.
- In many applications, the environment is not passive, for example, in the case of interaction with a human being. In fact, the human user can exhibit nonpassive dynamical behavior. However, from daily experience, it is known that the interaction of humans with passive objects is stable, unless the human operator intentionally tries to destabilize the system.

10.2.3 Simple 1-DoF Robot

To gain insight into the idea of impedance control, it is useful to start from single-input single-output systems. The results are then extended to multivariable and nonlinear systems.

Consider the simplified model of a rigid robot in Fig. 10.3. This model can be interpreted as the translational mechanical analog of a single-DoF robot with a revolute joint and an actuator which imposes a torque through a mechanical transmission.

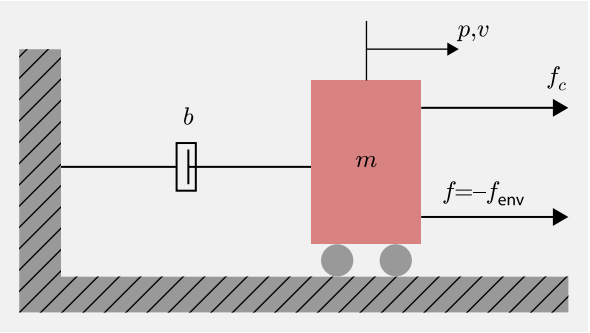

Fig. 10.3 Simplified model of a rigid robot

In the translational analogy, all quantities are reflected to the link side. In particular:

- $m > 0$ is the total mass, which is the analogous of the total inertia, sum of the inertia of the link and of the inertia of the motor reflected to the link side;
- $b \geq 0$ is the total viscous friction coefficient reflected to the link side; friction can be usually neglected in backdrivable robots, while it is often dominant in robots that are not backdrivable;
- p and $v = \dot{p}$ are respectively the position and velocity of the link (and of the environment), which are the translational analogous of the link angular position and velocity;
- f is the interaction force analogous to the interaction torque applied by the environment on the robot's link, which is opposite to force f_{env} applied by the robot on the environment;
- f_c is the control force analogous to the control torque.

Usually the mechanical transmissions, especially those with high transmission ratio, introduce nonlinear phenomena like Coulomb friction, stiction and backlash, which are difficult to model and are not considered here, but that further reduce backdrivability.

The equation of motion can be written in the form:

$$m\dot{v} + bv = f_c - f_{\text{env}}. \tag{10.4}$$

Impedance Control Without Force Feedback

Let us choose the control force f_c as

$$f_c = f_{PD} = k_d(p_d - p) + b_d(\dot{p}_d - \dot{p}), \tag{10.5}$$

corresponding to a position control of PD type, which can be interpreted as the force produced by a parallel spring and damper, with coefficients $k_d \geq 0$ and $b_d \geq 0$ respectively. The quantity p_d is a desired position, also known as *virtual* position,

corresponding to the rest position of the spring. The deviation of the virtual position from the actual position of the robot produces a force according to (10.5), which pushes or pulls the robot. In the absence of interaction with the environment (i.e., $f_{\text{env}} = 0$), the robot's position tends to follow the virtual position. If interaction occurs, the robot position deviates from the virtual position, which could be not reachable—for example, the environment is a wall and the virtual position is a point beyond the wall. This is the reason for the adjective *virtual*. The actual motion of the robot as well as the value of the interaction force depends, of course, on the desired position and desired velocity, but also on the parameters of the two interacting systems (controlled robot and environment) at the interaction port.

The interpretation of the interacting controlled robot–environment system in terms of impedance/admittance in this simple example can be achieved by expressing control law (10.5) in terms of velocities, i.e.,

$$f_c = f_{PI} = b_d(v_d - v) + k_d \int_0^t (v_d - v)d\tau, \tag{10.6}$$

with $v_d = \dot{p}_d$, representing a PI velocity control. In the Laplace domain it is

$$f_{PI} = Z_c(s)(v_d - v), \tag{10.7}$$

where

$$Z_c(s) = b_d + \frac{k_d}{s} \tag{10.8}$$

is the transfer function of the velocity controller. Similarly, the Laplace transform of the robot Eq. (10.4) gives:

$$Z_r(s)v = f_c - f_{\text{env}}, \tag{10.9}$$

where

$$Z_r(s) = ms + b \tag{10.10}$$

is the impedance of the uncontrolled robot. Using (10.9) with $f_c = f_{PI}$ in (10.7), the force $f = -f_{\text{env}}$ can be computed as

$$f = -f_{\text{env}} = Z(s)v - Z_c(s)v_d, \tag{10.11}$$

where

$$Z(s) = Z_r(s) + Z_c(s) = ms + b + b_d + \frac{k_d}{s} \tag{10.12}$$

is the apparent impedance of the controlled robot at the interaction port resulting from the parallel connection of the robot impedance $Z_r(s)$ with the control impedance $Z_c(s)$. The overall system can be represented as in Fig. 10.4, where $Y_{\text{env}}(s)$ is the admittance of the environment. One can easily verify (see Problem 10.1) that the transfer function in (10.12) is PR, hence $Z(s)$ is passive for all $b + b_d \geq 0$ and $k_d \geq 0$. Then, coupled stability is guaranteed in the event of interaction with any passive environment. The term depending on the desired velocity v_d in (10.11) is a feedforward contribution that is irrelevant for stability.

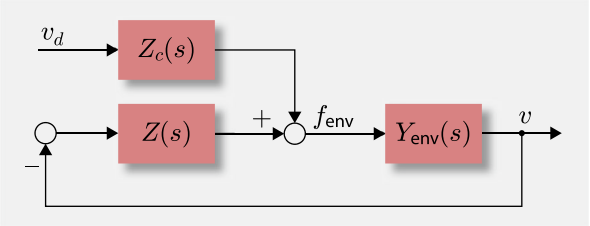

Fig. 10.4 Block diagram in the Laplace domain of the controlled robot (impedance $Z(s)$) interacting with the environment (admittance $Y_{\text{env}}(s)$)

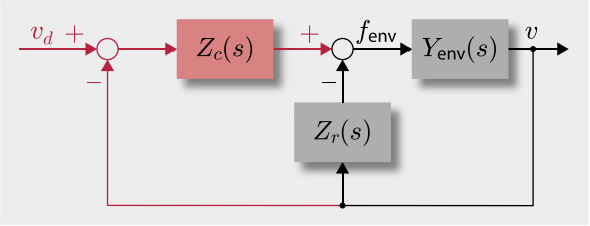

Fig. 10.5 Equivalent block diagram in the Laplace domain of the impedance control ($Z_c(s)$) for the robot ($Z_r(s)$) interacting with the environment ($Y_{\text{env}}(s)$)

An equivalent block diagram of the system is reported in Fig. 10.5, where different colors are used for the blocks modeling the control system, including the feedback signals, and those modeling the physical system (robot and environment) and the interaction variables (force and velocity).

In view of the expression (10.12) of the apparent impedance, it can be observed that:

- the mass m of the apparent impedance is equal to the mass of the robot and cannot be modified;
- since b is uncertain, the quantity b_d must always be set nonnegative to guarantee passivity, and then the overall damping cannot be lower than that of the uncontrolled robot.

In sum, to guarantee coupled stability, the apparent impedance $Z(s)$ can only be 'higher' than the impedance of the uncontrolled robot and an arbitrary apparent impedance cannot be achieved, in general. This is a drawback especially for high-impedance robots, namely, heavy robots or robots whose actuators are not backdrivable.

Impedance Control with Force Feedback

If a force sensor that allows measuring the force f_{env} is available, the following proportional control using force feedback can be adopted:

$$f_c = k_F(f_{PD} - f_{\text{env}}) + f_{\text{env}}, \tag{10.13}$$

where f_{PD} is the PD position control given in (10.5). The latter can also be replaced by the equivalent PI velocity control f_{PI} in (10.6). The last term in (10.13), which (ideally) allows canceling out the interaction force f_{env}, could also be omitted with

minor changes in the analysis. Overall, the controller consists of an 'inner' force feedback loop and an 'outer' position (or velocity) feedback loop.

By replacing control law (10.13) into the equation of the robot (10.4), the computation of the force f_{env} from the velocity v in the Laplace domain yields the same Eq. (10.11), with apparent impedance

$$Z(s) = \frac{1}{k_F} Z_r(s) + Z_c(s) = \frac{m}{k_F} s + \frac{b}{k_F} + b_d + \frac{k_d}{s}, \tag{10.14}$$

where $Z_c(s)$ and $Z_r(s)$ are defined in (10.8) and (10.10) respectively. The controlled robot in interaction with the environment can be represented by the same block diagram in Fig. 10.4, with the apparent robot's impedance (10.14). It is worth observing what follows.

- The inner force feedback loop $-k_F f_{\text{env}}$ in (10.13) allows reshaping the robot apparent impedance as $Z_r(s)/k_F$ and, in particular, achieve a desired mass setting the proportional gain as $k_F = m/m_d$.
- The outer position control loop f_{PD} in (10.5)—or the equivalent velocity control loop f_{PI} in (10.6)—allows achieving a desired stiffness k_d and an additional desired damping b_d.
- In the presence of intrinsic structural compliance of the robot (i.e., flexibility in the links or elasticity in the joints, as is often the case in cobots) it can be found that the gain k_F must be set in the interval $[0, 1]$ to guarantee passivity (see Problem 10.3). On the other hand, passivity is always guaranteed, also in the presence of structural compliance, if impedance control without force feedback is adopted (see Problem 10.2).

Admittance Control

The idea of admittance control is that of exploiting the motion control loop of the robot in free space, which is designed to make the robot as fast and accurate as possible while rejecting friction and all external disturbances (including interaction forces). It follows that the controlled robot behaves like a desired admittance imposing a velocity on the environment, modeled as an impedance. The desired force–velocity relation (i.e., the desired, or apparent, admittance) for the controlled robot at the interaction port is obtained by closing an outer force control loop around the inner motion control loop, as in Fig. 10.6, where $C_f(s)$ is the transfer function of the force controller, $C_v(s)$ is the transfer function of the velocity controller, $Y_r(s) = 1/Z_r(s)$ is the admittance of the robot, and $Z_{\text{env}}(s) = 1/Y_{\text{env}}(s)$ is the impedance of the environment. In Fig. 10.6 different colors are used to distinguish the blocks representing the controllers and the measured signals from the blocks representing the physical systems and the interaction variables.

In the absence of interaction ($f_{\text{env}} = 0$), the outer force control loop is inactive and the robot follows the desired velocity v_d, i.e., $v \approx v_d$. When an interaction occurs, to study coupled stability, it is necessary to calculate the transfer function from the force $f = -f_{\text{env}}$ to the velocity v, i.e., the admittance of the controlled robot, assuming

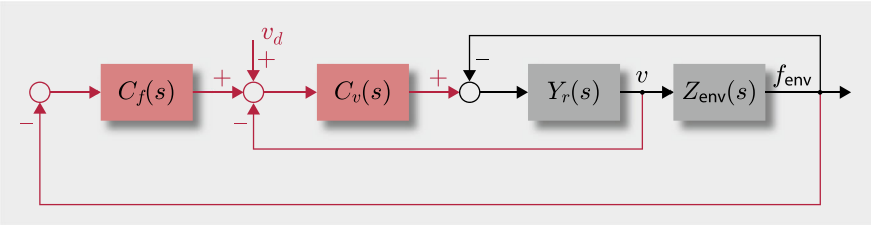

Fig. 10.6 Block diagram of admittance control

$v_d = 0$, being v_d irrelevant for stability. Namely, it is $v = -Y(s) f_{\text{env}} = Y(s) f$ with

$$Y(s) = \frac{C_v(s) Y_r(s)}{1 + C_v(s) Y_r(s)} C_f(s) + \frac{Y_r(s)}{1 + C_v(s) Y_r(s)}. \tag{10.15}$$

The admittance $Y(s)$ can be computed from the block diagram of Fig. 10.6 by opening the loop at the input of impedance $Z_{\text{env}}(s)$ and computing the output velocity v from the input force $f = -f_{\text{env}}$ (see Problem 10.4). In case of a high-gain velocity controller, the second term of the sum (10.15) can be neglected. This term could also be canceled by adding a force feedback to the control input that (ideally) cancels the interaction force f_{env} as in the control law (10.13). Moreover, in the bandwidth of the velocity control loop, the following approximation holds:

$$Y(s) \approx C_f(s), \tag{10.16}$$

and therefore, by setting $C_f(s) = Y_d(s)$, any kind of passive desired admittance can be achieved, as that corresponding to a mass–spring–damper system

$$Y_d(s) = \frac{1}{m_d s + b_d + k_d / s}, \tag{10.17}$$

with all the possible combinations of null and nonnull (strictly positive) parameters. For instance, a pure stiffness, a pure damping, as well as a pure mass behavior can be rendered, and this is not possible with impedance control, with or without force feedback.

However, the approximation (10.16) can be inaccurate and, in any case, it does not hold at all frequencies but at most within the bandwidth of the velocity control loop. At these frequencies the apparent admittance can be made close to the desired one; otherwise, the dynamics of the inner motion control loop cannot be neglected and the passivity of the apparent admittance is not always guaranteed (see Problem 10.5).

10.2.4 Multi-DoF Robots

The impedance control approach can be extended to multi-DoF robots, by taking advantage of the passivity of robot dynamics (see Sect. 5.3.1).

Compliance Control

The basic control law that can be used to ensure a passive behavior of a robot interacting with the environment is known as *compliance control*.

The dynamic model of a n-joint robot interacting with the environment can be written as

$$\boldsymbol{M}(\boldsymbol{q})\ddot{\boldsymbol{q}} + \boldsymbol{c}(\boldsymbol{q}, \dot{\boldsymbol{q}}) + \boldsymbol{B}_v\dot{\boldsymbol{q}} + \boldsymbol{g}(\boldsymbol{q}) = \boldsymbol{\tau} - \boldsymbol{\tau}_{\text{env}} \tag{10.18}$$

where the $\boldsymbol{\tau}_{\text{env}} = -\boldsymbol{\tau}_{\text{int}}$ is the vector of the joint torques resulting from the interaction forces applied by the robot to the environment, and contact may happen in any point of the robot's body. The model (10.18) also includes viscous friction $-\boldsymbol{B}_v\dot{\boldsymbol{q}}$, as in the 1-DoF case.[3]

Joint-space compliance control is based on PD control with gravity cancellation in joint space (6.31), i.e.,

$$\boldsymbol{\tau} = \boldsymbol{K}_P\boldsymbol{e} - \boldsymbol{K}_D\dot{\boldsymbol{q}} + \boldsymbol{g}(\boldsymbol{q}), \tag{10.19}$$

being $\boldsymbol{e} = \boldsymbol{q}_d - \boldsymbol{q}$ the joint position error. Using this control, Eq. (10.18) can be rewritten in the form

$$-\boldsymbol{\tau}_{\text{env}} = \boldsymbol{M}(\boldsymbol{q})\ddot{\boldsymbol{q}} + \boldsymbol{c}(\boldsymbol{q}, \dot{\boldsymbol{q}}) + (\boldsymbol{B}_v + \boldsymbol{K}_D)\dot{\boldsymbol{q}} - \boldsymbol{K}_P\boldsymbol{e}. \tag{10.20}$$

This equation can be interpreted as a nonlinear impedance with input $\dot{\boldsymbol{q}}$ and output $-\boldsymbol{\tau}_{\text{env}}$ which generalizes the single-input single-output linear impedance in the Laplace domain defined by (10.11) and (10.12). In particular, it represents a configuration-dependent mechanical impedance of mass–spring–damper type in joint space, with inertia (mass) matrix $\boldsymbol{M}(\boldsymbol{q})$, adjustable damping $\boldsymbol{B}_v + \boldsymbol{K}_D$, and adjustable stiffness $\boldsymbol{K}_P$.

To continue the analogy with the linear case, note that, by ignoring the gravity that is canceled by the control, the apparent impedance (10.20) can be seen as the parallel interconnection of the robot impedance and the control impedance. The robot impedance (10.18) defines a passive system from $\dot{\boldsymbol{q}}$ to $\boldsymbol{\tau}$ with storage function

$$V_1 = \frac{1}{2}\dot{\boldsymbol{q}}^T\boldsymbol{M}(\boldsymbol{q})\dot{\boldsymbol{q}},$$

being

$$\dot{V}_1 = \boldsymbol{\tau}^T\dot{\boldsymbol{q}} - \dot{\boldsymbol{q}}^T\boldsymbol{B}_v\dot{\boldsymbol{q}},$$

obtained by replacing $\ddot{\boldsymbol{q}}$ computed from (10.18) with $\boldsymbol{g} = \boldsymbol{0}$ and $\boldsymbol{\tau}_{\text{env}} = \boldsymbol{0}$ into the time derivative of V_1, and using the passivity property (5.55) of the robot's dynamic

[3] Other friction effects, if present, can be regarded as unstructured uncertainties and are ignored here.

model. By integrating the above equation, the following inequality holds:

$$V_1(t) - V_1(0) \leq \int_0^t \boldsymbol{\tau}^T \dot{\boldsymbol{q}}\, d\tau - \lambda'_m \int_0^t \dot{\boldsymbol{q}}^T \dot{\boldsymbol{q}}\, d\tau,$$

being $\lambda'_m \geq 0$ the minimum eigenvalue of the positive semi-definite matrix $\boldsymbol{B}_v$. This proves that the robot's dynamics is passive and is input strictly passive if $\lambda'_m > 0$. Regarding control (10.19), it defines a passive impedance from $\dot{\boldsymbol{q}}$ to $\boldsymbol{\tau}$ with storage function

$$V_2 = \frac{1}{2} \boldsymbol{e}^T \boldsymbol{K}_P \boldsymbol{e},$$

being

$$\dot{V}_2 = \boldsymbol{\tau}^T \dot{\boldsymbol{q}} - \dot{\boldsymbol{q}}^T \boldsymbol{K}_d \dot{\boldsymbol{q}},$$

obtained by replacing $\boldsymbol{e}$ computed from (10.19) with $\boldsymbol{g} = \boldsymbol{0}$ into the time derivative of V_2. By integrating the above equation, the following inequality holds:

$$V_2(t) - V_2(0) \leq \int_0^t \boldsymbol{\tau}^T \dot{\boldsymbol{q}}\, d\tau - \lambda''_m \int_0^t \dot{\boldsymbol{q}}^T \dot{\boldsymbol{q}}\, d\tau,$$

being $\lambda''_m > 0$ the minimum eigenvalue of the positive definite matrix $\boldsymbol{K}_D$. This proves that the control is input strictly passive.

The passivity of the apparent impedance (10.20) can be proven using the storage function $V = V_1 + V_2$, which coincides with the Lyapunov candidate in (6.28). Computing the time derivative of V along the trajectories of the system (10.20) gives

$$\dot{V} = (-\boldsymbol{\tau}_{\text{env}})^T \dot{\boldsymbol{q}} - \dot{\boldsymbol{q}}^T (\boldsymbol{B}_v + \boldsymbol{K}_D) \dot{\boldsymbol{q}} \leq (-\boldsymbol{\tau}_{\text{env}})^T \dot{\boldsymbol{q}} - \lambda_m \dot{\boldsymbol{q}}^T \dot{\boldsymbol{q}}, \tag{10.21}$$

being $\lambda_m > 0$ the minimum eigenvalue of the positive definite (usually diagonal) matrix $\boldsymbol{B}_v + \boldsymbol{K}_D$. Therefore, the following inequality holds:

$$V(t) - V(0) \leq \int_0^t (-\boldsymbol{\tau}_{\text{env}})^T \dot{\boldsymbol{q}}\, d\tau - \lambda_m \int_0^t \dot{\boldsymbol{q}}^T \dot{\boldsymbol{q}}\, d\tau, \tag{10.22}$$

showing that system (10.20) is input strictly passive. This means that coupled stability is guaranteed in the event of interaction with any passive environment (see Appendix D.3).

If interaction occurs at a specific (known) location of the robot's body, e.g., on the end-effector, identified by the task vector $\boldsymbol{y} \in \mathbb{R}^m$, the torque reflected at the joints is $\boldsymbol{\tau}_{\text{env}} = \boldsymbol{J}^T(\boldsymbol{q}) \boldsymbol{\gamma}_{\text{env}}$, being $\boldsymbol{\gamma}_{\text{env}}$ the generalized force applied by the robot to the environment performing work on the task coordinates $\boldsymbol{y}$, and $\boldsymbol{J}(\boldsymbol{q})$ the corresponding task Jacobian, also referred to as *contact Jacobian*. Moreover, for control design and

analysis it is useful to consider the task-space dynamic model (5.132) defined as

$$\boldsymbol{\Lambda}(\boldsymbol{q})\ddot{\boldsymbol{y}} + \boldsymbol{\psi}(\boldsymbol{q}, \dot{\boldsymbol{q}}) + \boldsymbol{\beta}(\boldsymbol{q}, \dot{\boldsymbol{q}}) + \boldsymbol{\eta}(\boldsymbol{q}) = \boldsymbol{\gamma} - \boldsymbol{\gamma}_{\text{env}}, \tag{10.23}$$

being $\boldsymbol{\Lambda}(\boldsymbol{q})$, $\boldsymbol{\psi}(\boldsymbol{q}, \dot{\boldsymbol{q}})$, $\boldsymbol{\eta}(\boldsymbol{q})$ and $\boldsymbol{\gamma}$ the inertia matrix, the vector of centrifugal and Coriolis effects, the gravity contribution and the control input, respectively, reflected in task space. Moreover, the vector $\boldsymbol{\beta}(\boldsymbol{q}, \dot{\boldsymbol{q}}) = (\boldsymbol{J}_{\boldsymbol{M}}^{\dagger}(\boldsymbol{q}))^{T} \boldsymbol{B}_{v} \dot{\boldsymbol{q}}$ is the contribution of joint friction reflected in the task space. For simplicity, it is assumed $m = n$, i.e., the case of nonredundant robots.

Task-space compliance control is based on the PD control with gravity cancellation in task space (6.81), which can be written in the form

$$\boldsymbol{\tau} = \boldsymbol{J}^{T}(\boldsymbol{q})\boldsymbol{\gamma} + \boldsymbol{g}(\boldsymbol{q}), \tag{10.24}$$

with

$$\boldsymbol{\gamma} = -\boldsymbol{K}_{D}\dot{\boldsymbol{y}} + \boldsymbol{K}_{P}\boldsymbol{e}_{\boldsymbol{y}}, \tag{10.25}$$

being $\dot{\boldsymbol{y}} = \boldsymbol{J}(\boldsymbol{q})\dot{\boldsymbol{q}}$ and $\boldsymbol{e}_{\boldsymbol{y}} = \boldsymbol{y}_{d} - \boldsymbol{y}$ the task-space error with respect to a virtual pose $\boldsymbol{y}_{d}$. To compute the closed-loop equation, the control torque (10.24) with (10.25) must be replaced into the joint-space dynamic model (10.18). Alternatively, the task-space control input (10.25) can be directly replaced into the task-space dynamic model (10.23) without the gravity contribution, because it is canceled by the control torque (10.24). The result is the equation

$$-\boldsymbol{\gamma}_{\text{env}} = \boldsymbol{\Lambda}(\boldsymbol{q})\ddot{\boldsymbol{y}} + \boldsymbol{\psi}(\boldsymbol{q}, \dot{\boldsymbol{q}}) + \boldsymbol{\beta}(\boldsymbol{q}, \dot{\boldsymbol{q}}) + \boldsymbol{K}_{D}\dot{\boldsymbol{y}} - \boldsymbol{K}_{P}\boldsymbol{e}_{\boldsymbol{y}}, \tag{10.26}$$

which is a multivariable, nonlinear and configuration-dependent mechanical impedance with input $\dot{\boldsymbol{y}}$ and output $-\boldsymbol{\gamma}_{\text{env}}$. In particular, it represents a mass–spring–damper system in task space, with inertia matrix $\boldsymbol{\Lambda}(\boldsymbol{q})$, adjustable damping $\boldsymbol{K}_{D}$ and adjustable stiffness $\boldsymbol{K}_{P}$. It can be shown that the above impedance equation is input strictly passive (see also Example 10.2 and Problem 10.7), and thus coupled stability is guaranteed in case of interaction with any passive environment.

Note that, for both joint-space and task-space compliance control, to ensure satisfactory performance during interaction, the elements of matrices $\boldsymbol{K}_{D}$ and $\boldsymbol{K}_{P}$ should be properly set, considering that it is not possible to modify the natural inertia of the robot, nor the joint friction torques. Therefore, the performance during the interaction can be poor in case that the natural robot's inertia and the joint friction are dominant with respect to the desired damping $\boldsymbol{K}_{D}$ and stiffness $\boldsymbol{K}_{P}$. This happens, for example, when trying to impose a low impedance to a bulky industrial robot.

A partial solution to this problem can be that of using force feedback, as in the single-input single-output case (10.13). For example, if the interaction is on the end-effector and a wrist force/torque sensor is available to measure the interaction force, then the PD control with gravity cancellation in task space (10.24), (10.25) can be modified by replacing $\boldsymbol{\gamma}$ in (10.24) with

$$\boldsymbol{\gamma}' = k_{F}(\boldsymbol{\gamma} - \boldsymbol{\gamma}_{\text{env}}) + \boldsymbol{\gamma}_{\text{env}}, \tag{10.27}$$

with γ given in (10.25), and $k_F > 0$ is a suitable control gain. This yields the new task-space impedance equation

$$-\gamma_{\text{env}} = k_F^{-1}\big(\boldsymbol{\Lambda}(\boldsymbol{q})\ddot{\boldsymbol{y}} + \boldsymbol{\psi}(\boldsymbol{q},\dot{\boldsymbol{q}}) + \boldsymbol{\beta}(\boldsymbol{q},\dot{\boldsymbol{q}})\big) + \boldsymbol{K}_D\dot{\boldsymbol{y}} - \boldsymbol{K}_P\boldsymbol{e}_{\boldsymbol{y}}, \tag{10.28}$$

showing that the inertia, centrifugal, Coriolis, and joint friction contributions of the robot are scaled by a factor k_F. In principle, high values can be set for the gain k_F, in order to reduce these dynamic contributions and, together with the gain matrices $\boldsymbol{K}_D$ and $\boldsymbol{K}_P$, modify the robot's apparent impedance as desired. However, as observed in the single-input single-output case, in the presence of structural flexibility in the joint transmissions or in the links of the robot, the value of k_F must be kept small to preserve passivity.

All the control strategies presented in this section allow imposing to the robot a compliant behavior described by an impedance with adjustable *compliance*[4] $\boldsymbol{K}_P^{-1}$ and, in part, adjustable damping through matrix $\boldsymbol{K}_D$. This is the reason of the name *compliance control*.

Example 10.2 Consider the 2R planar arm in Fig. 10.7, whose tip is in contact with a purely frictionless elastic plane. The robot task is the end-effector position, described by vector

$$\boldsymbol{y}_e = \begin{pmatrix} x_e \\ z_e \end{pmatrix}.$$

The interaction force γ_{env} applied by the robot to the environment is opposed to the elastic force produced by the deformation $\gamma_{\text{el}} = -\boldsymbol{K}(\boldsymbol{y}_e - \boldsymbol{y}_r)$, namely:

$$\gamma_{\text{env}} = -\gamma_{\text{el}} = \boldsymbol{K}(\boldsymbol{y}_e - \boldsymbol{y}_r) = \begin{pmatrix} k(x_e - x_r) \\ 0 \end{pmatrix},$$

where $\boldsymbol{y}_r = (x_r, z_r)$ is a point of the plane at the equilibrium (i.e., with null elastic force) and $\boldsymbol{K} = \text{diag}\{k, 0\}$ is the environment stiffness matrix. All the quantities are referred to the base frame O–x_0z_0. Due to the simple geometry of the problem, the vertical component of the contact force is always null, and passivity can be analyzed considering the scalar equation

$$f_{\text{env}} = k(x_e - x_r),$$

being f_{env} the horizontal component of the contact force. The above relationship can be seen as an impedance with input velocity $\dot{x}_e$, output force f_{env}, and transfer function k/s, as well as an admittance with transfer function s/k and inverted causality. Both transfer functions are PR, and thus the environment is passive. Therefore, the equation in vector form defines a passive admittance between the input force γ_{env}

[4] Compliance matrix is the inverse of stiffness matrix.

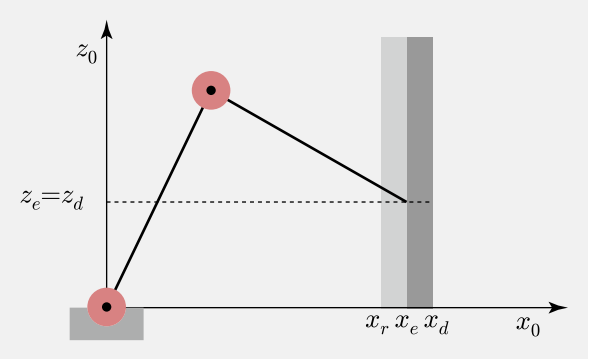

Fig. 10.7 2R planar arm in contact with an elastically compliant plane

and the output velocity $\dot{\boldsymbol{y}}_e$. It is straightforward to show that the elastic energy

$$V_1 = \frac{1}{2}(\boldsymbol{y}_e - \boldsymbol{y}_r)^T \boldsymbol{K}(\boldsymbol{y}_e - \boldsymbol{y}_r)$$

is the storage function of this passive system.

By using the compliance control law (10.24) with (10.25), the controlled robot can be seen as the nonlinear impedance with input $\dot{\boldsymbol{y}}_e$ and output $-\boldsymbol{\gamma}_{\text{env}}$ described by equation

$$\boldsymbol{\Lambda}(\boldsymbol{q})\ddot{\boldsymbol{y}}_e + \boldsymbol{\Gamma}(\boldsymbol{q}, \dot{\boldsymbol{q}})\dot{\boldsymbol{y}}_e + \boldsymbol{\beta}(\boldsymbol{q}, \dot{\boldsymbol{q}}) + k_D\dot{\boldsymbol{y}}_e - k_P(\boldsymbol{y}_d - \boldsymbol{y}_e) = -\boldsymbol{\gamma}_{\text{env}}, \qquad (10.29)$$

where $\boldsymbol{y}_d = (x_d, z_d)$ is the robot virtual position, $\boldsymbol{\Gamma}(\boldsymbol{q}, \dot{\boldsymbol{q}})$ is the matrix of centrifugal and Coriolis terms projected in task space defined in (5.143) and, for simplicity, $\boldsymbol{K}_D = k_D\boldsymbol{I}$ and $\boldsymbol{K}_P = k_P\boldsymbol{I}$. The passivity can be analyzed using the storage function

$$V_2 = \frac{1}{2}\dot{\boldsymbol{y}}_e^T\boldsymbol{\Lambda}(\boldsymbol{q})\dot{\boldsymbol{y}}_e + \frac{1}{2}k_P(\boldsymbol{y}_d - \boldsymbol{y}_e)^T(\boldsymbol{y}_d - \boldsymbol{y}_e),$$

whose time derivative along the trajectories of (10.29) is

$$\dot{V}_2 = (-\boldsymbol{\gamma}_{\text{env}})^T\dot{\boldsymbol{y}}_e - \dot{\boldsymbol{q}}^T\boldsymbol{B}_v\dot{\boldsymbol{q}} - k_D\dot{\boldsymbol{y}}_e^T\dot{\boldsymbol{y}}_e$$

from which

$$V_2(t) - V_2(0) \leq \int_0^t (-\boldsymbol{\gamma}_{\text{env}})^T\dot{\boldsymbol{y}}_e\, d\tau - k_D\int_0^t \dot{\boldsymbol{y}}_e^T\dot{\boldsymbol{y}}_e\, d\tau,$$

being $\dot{\boldsymbol{q}}^T\boldsymbol{B}_v\dot{\boldsymbol{q}} \geq 0$. Therefore the controlled robot is an input strictly passive system and the coupled system is also passive, at least. The storage functions V_1 and V_2 are useful to prove asymptotic stability of the equilibrium of the coupled system

$$\boldsymbol{\Lambda}(\boldsymbol{q})\ddot{\boldsymbol{y}}_e + \boldsymbol{\Gamma}(\boldsymbol{q}, \dot{\boldsymbol{q}})\dot{\boldsymbol{y}}_e + \boldsymbol{\beta}(\boldsymbol{q}, \dot{\boldsymbol{q}}) + k_D\dot{\boldsymbol{y}}_e - k_P(\boldsymbol{y}_d - \boldsymbol{y}_e) + \boldsymbol{K}(\boldsymbol{y}_e - \boldsymbol{y}_r) = \boldsymbol{0}.$$

At the equilibrium, the end-effector velocity is null, i.e., $\dot{\boldsymbol{y}}_e = \mathbf{0}$, and the end-effector position is the solution $\boldsymbol{y}_\infty$ of equation

$$k_P(\boldsymbol{y}_d - \boldsymbol{y}_\infty) - \boldsymbol{K}(\boldsymbol{y}_\infty - \boldsymbol{y}_r) = \mathbf{0},$$

namely

$$\boldsymbol{y}_\infty = \begin{pmatrix} \dfrac{k_P x_d + k x_r}{k_P + k} \\ z_d \end{pmatrix},$$

which is also the unique minimum of the nonnegative function

$$V_3 = \frac{1}{2}(\boldsymbol{y}_e - \boldsymbol{y}_r)^T \boldsymbol{K}(\boldsymbol{y}_e - \boldsymbol{y}_r) + \frac{1}{2} k_P (\boldsymbol{y}_d - \boldsymbol{y}_e)^T (\boldsymbol{y}_d - \boldsymbol{y}_e).$$

The asymptotic stability of the equilibrium ($\dot{\boldsymbol{y}}_e = \mathbf{0}$, $\boldsymbol{y}_e = \boldsymbol{y}_\infty$) for the coupled system can be shown with the Lyapunov candidate

$$V = V_1(\boldsymbol{y}_e) + V_2(\boldsymbol{y}_e, \dot{\boldsymbol{y}}_e) - V_3(\boldsymbol{y}_\infty) > 0,$$

which is positive definite in any neighborhood of the equilibrium. The time derivative of V along the trajectories of the system is

$$\dot{V} = -\dot{\boldsymbol{q}}^T \boldsymbol{B}_v \dot{\boldsymbol{q}} - k_D \dot{\boldsymbol{y}}_e^T \dot{\boldsymbol{y}}_e.$$

Since $\dot{V}$ is negative semi-definite, the coupled system is asymptotically stable in the sense of Lyapunov, provided that $k_P > 0$ and $k_D > 0$. In principle, k_D could be also null in the presence of joint friction, without losing asymptotic stability.

The contact force applied by the robot to the environment at equilibrium has the form

$$\boldsymbol{\gamma}_\infty = \begin{pmatrix} f_\infty \\ 0 \end{pmatrix} = \begin{pmatrix} \dfrac{k_P k}{k_P + k}(x_d - x_r) \\ 0 \end{pmatrix}.$$

With reference to position $\boldsymbol{y}_\infty$ at equilibrium, the arm tip reaches the vertical coordinate z_d, since the interaction force is null along the vertical direction. As for the horizontal direction, the presence of the elastic plane imposes that the arm can move as far as it reaches the coordinate $x_\infty < x_d$. The value of the horizontal contact force at the equilibrium is related to the difference between the virtual position x_d and the position x_r of the undeformed plane by an equivalent stiffness coefficient which is given by the parallel composition of the stiffness coefficients of the two interacting systems. Hence, the arm stiffness and environment stiffness influence the resulting equilibrium configuration. In the case when

$$k_P / k \gg 1,$$

it is

$$x_\infty \approx x_d \qquad f_\infty = k(x_\infty - x_r) \approx k(x_d - x_r)$$

and thus the arm prevails over the environment, in that the plane complies almost up to x_d. Thus f_∞ is the force required to produce the displacement $x_\infty - x_r$ of the environment from the undeformed position x_r, which depends only on the stiffness, or compliance, of the environment (passive stiffness or compliance). In the opposite case

$$k_P/k \ll 1,$$

it is

$$x_\infty \approx x_r \qquad f_\infty \approx k_P(x_d - x_r) \approx -k_P(x_\infty - x_d)$$

and thus the environment prevails over the arm which remains stuck at x_r. In this case f_∞ is the elastic force produced by the controlled arm which behaves like a spring of stiffness k_P (compliance k_P^{-1}), in response to the displacement $x_\infty - x_d$ from the virtual position x_d (active stiffness or compliance). ■

Impedance Control

If the dynamics of the robot is known and can be used for control purposes, it is possible to improve the rendering of the desired impedance or admittance of the controlled robot at the interaction port. For simplicity, only the case of nonredundant robots is considered.

In general, model-based compensation is not very effective for joint friction, which is difficult to model and can be better rejected by feedback control, or by a combination of feedback and model-based compensation. Hence, as an outcome of the analysis carried out for the simplified 1-DoF case, it is argued that impedance control is more effective in case that joint friction is negligible. If this is not the case, as for robots that are not backdrivable, it is advisable to adopt an admittance control approach.

Assuming that friction is negligible, i.e., $\boldsymbol{\beta}(\boldsymbol{q}, \dot{\boldsymbol{q}}) \approx \mathbf{0}$ in (10.23), the PD control with gravity cancellation in task space (10.24) can be modified by adding a model-based and feedforward contribution to the control input in (10.25), namely choosing $\boldsymbol{\gamma}$ in (10.24) as

$$\boldsymbol{\gamma} = \boldsymbol{\Lambda}(\boldsymbol{q})\ddot{\boldsymbol{y}}_d + \boldsymbol{\Gamma}(\boldsymbol{q}, \dot{\boldsymbol{q}})\dot{\boldsymbol{y}}_d + \boldsymbol{K}_D\dot{\boldsymbol{e}}_{\boldsymbol{y}} + \boldsymbol{K}_P\boldsymbol{e}_{\boldsymbol{y}} \tag{10.30}$$

where $\boldsymbol{\Gamma}(\boldsymbol{q}, \dot{\boldsymbol{q}})$ is the matrix of centrifugal and Coriolis terms defined in (5.143), and a time-varying task-space desired trajectory $\boldsymbol{y}_d(t)$ is assigned. This control law is the task-space counterpart of the joint-space inverse dynamics control law (6.50). In case of regulation to a constant $\boldsymbol{y}_d$, the PD control with gravity cancellation in task space (10.24), (10.25) is recovered.

Substituting (10.24) with (10.30) in (10.18) with $\boldsymbol{B}_v = \boldsymbol{O}$ leads to

$$\boldsymbol{\Lambda}(\boldsymbol{q})\ddot{\boldsymbol{e}}_{\boldsymbol{y}} + \boldsymbol{\Gamma}(\boldsymbol{q}, \dot{\boldsymbol{q}})\dot{\boldsymbol{e}}_{\boldsymbol{y}} + \boldsymbol{K}_D\dot{\boldsymbol{e}}_{\boldsymbol{y}} + \boldsymbol{K}_P\boldsymbol{e}_{\boldsymbol{y}} = \boldsymbol{\gamma}_{\text{env}}, \tag{10.31}$$

representing the dynamics of the task-space error $\boldsymbol{e}_{\boldsymbol{y}}(t) = \boldsymbol{y}_d(t) - \boldsymbol{y}(t)$. This equation can also be easily computed by replacing (10.30) into the task-space dynamic model (10.23) with null friction and gravity. In the absence of interaction ($\boldsymbol{\gamma}_{\text{env}} = \mathbf{0}$), it

is possible to prove asymptotic convergence to zero of the errors $\boldsymbol{e}_{\boldsymbol{y}}(t)$ and $\dot{\boldsymbol{e}}_{\boldsymbol{y}}(t)$, provided that singularities are avoided during the motion. Therefore, in free space, the controller guarantees the tracking of the desired trajectory $\boldsymbol{y}_d(t)$ as for the joint-space counterpart.

In the presence of interaction ($\boldsymbol{\gamma}_{\text{env}} \neq \boldsymbol{0}$), trajectory tracking is no longer achieved and $\boldsymbol{y}_d(t)$ becomes a virtual trajectory. In this case, if $\boldsymbol{y}_d$ is kept constant, using the nonnegative storage function

$$V = \frac{1}{2}\dot{\boldsymbol{y}}^T \boldsymbol{\Lambda}(\boldsymbol{q})\dot{\boldsymbol{y}} + \frac{1}{2}\boldsymbol{e}_{\boldsymbol{y}}^T \boldsymbol{K}_P \boldsymbol{e}_{\boldsymbol{y}}. \tag{10.32}$$

It is possible to prove that the controlled robot, described by the nonlinear impedance

$$-\boldsymbol{\gamma}_{\text{env}} = \boldsymbol{\Lambda}(\boldsymbol{q})\ddot{\boldsymbol{y}} + \boldsymbol{\Gamma}(\boldsymbol{q}, \dot{\boldsymbol{q}})\dot{\boldsymbol{y}} + \boldsymbol{K}_D\dot{\boldsymbol{y}} - \boldsymbol{K}_P\boldsymbol{e}_{\boldsymbol{y}},$$

with input $\dot{\boldsymbol{y}}$ and output $-\boldsymbol{\gamma}_{\text{env}}$, is passive. Hence, coupled stability is ensured if the environment is passive.

In sum, the advantage of the PD control with model-based feedforward (10.24), (10.30), with respect to the simple PD control (10.24), (10.25) considered in the previous section, is the improved motion tracking capability during free motion. The main limitation of both approaches is that the physical inertia of the robot projected in task space cannot be modified, and thus the performance of the controlled system, both in free space or during contact with the environment, depends on the robot configuration, making it difficult to choose the gain matrices $\boldsymbol{K}_D$ and $\boldsymbol{K}_P$.

This problem can be overcome if the measurement of the interaction force is available and can be used by the controller together with model-based compensation torques. The resulting impedance control law can be equivalently formulated in joint space or task space and derives from the feedback linearization control in task space presented in Sect. 6.5.2.

For the purpose of the analysis, the control torque is conveniently written in the form

$$\boldsymbol{\tau} = \boldsymbol{J}^T(\boldsymbol{q})\boldsymbol{\gamma} + \boldsymbol{n}(\boldsymbol{q}, \dot{\boldsymbol{q}}), \tag{10.33}$$

where the torque $\boldsymbol{n}(\boldsymbol{q}, \dot{\boldsymbol{q}})$, defined in (6.41) compensates the effects of centrifugal, Coriolis and gravity contributions. Control force $\boldsymbol{\gamma}$ in (10.33) is set to

$$\boldsymbol{\gamma} = \boldsymbol{\Lambda}(\boldsymbol{q})\big(\boldsymbol{a}_{\boldsymbol{y}} - \dot{\boldsymbol{J}}(\boldsymbol{q})\dot{\boldsymbol{q}}\big) + \boldsymbol{\gamma}_{\text{env}}, \tag{10.34}$$

where $\boldsymbol{a}_{\boldsymbol{y}}$ a new control input with the meaning of task-space acceleration and the measured interaction force $\boldsymbol{\gamma}_{\text{env}}$ is used to cancel out the interaction force. Plugging (10.33) with (10.34) into the joint-space dynamic model (10.18) and neglecting friction torques, the following expression for the joint acceleration is obtained:

$$\ddot{\boldsymbol{q}} = \boldsymbol{M}^{-1}(\boldsymbol{q})\boldsymbol{J}^T(\boldsymbol{q})\boldsymbol{\Lambda}(\boldsymbol{q})\big(\boldsymbol{a}_{\boldsymbol{y}} - \dot{\boldsymbol{J}}(\boldsymbol{q})\dot{\boldsymbol{q}}\big).$$

Multiplying from the left both sides of the above equation by the Jacobian matrix $\boldsymbol{J}(\boldsymbol{q})$, and taking into account the expression (5.131) of the task-space inertia and

the expression (5.128) of the task-space acceleration, gives

$$\ddot{\boldsymbol{y}} = \boldsymbol{a}_{\boldsymbol{y}}. \tag{10.35}$$

Hence, setting

$$\boldsymbol{a}_{\boldsymbol{y}} = \ddot{\boldsymbol{y}}_d + \boldsymbol{M}_d^{-1}\left(\boldsymbol{K}_D\dot{\boldsymbol{e}}_{\boldsymbol{y}} + \boldsymbol{K}_P\boldsymbol{e}_{\boldsymbol{y}} - \boldsymbol{\gamma}_{\text{env}}\right), \tag{10.36}$$

with $\boldsymbol{e}_{\boldsymbol{y}}(t) = \boldsymbol{y}_d(t) - \boldsymbol{y}(t)$, the following equation is obtained:

$$\boldsymbol{M}_d\ddot{\boldsymbol{e}}_{\boldsymbol{y}} + \boldsymbol{K}_D\dot{\boldsymbol{e}}_{\boldsymbol{y}} + \boldsymbol{K}_P\boldsymbol{e}_{\boldsymbol{y}} = \boldsymbol{\gamma}_{\text{env}}. \tag{10.37}$$

Differently from (10.31), the above equation is linear and configuration independent. In the absence of interaction ($\boldsymbol{\gamma}_{\text{env}} = \boldsymbol{0}$), the exponential stability of the equilibrium ($\dot{\boldsymbol{e}}_{\boldsymbol{y}} = \boldsymbol{0}$, $\boldsymbol{e}_{\boldsymbol{y}} = \boldsymbol{0}$) is ensured for positive definite matrices $\boldsymbol{M}_d$, $\boldsymbol{K}_D$ and $\boldsymbol{K}_P$. In the presence of interaction ($\boldsymbol{\gamma}_{\text{env}} \neq \boldsymbol{0}$), by ignoring the desired trajectory as in the linear case, the following equation is derived from (10.37):

$$-\boldsymbol{\gamma}_{\text{env}} = \boldsymbol{M}_d\ddot{\boldsymbol{y}} + \boldsymbol{K}_D\dot{\boldsymbol{y}} + \boldsymbol{K}_P\boldsymbol{y},$$

representing a mechanical impedance with input $\dot{\boldsymbol{y}}$ and output $-\boldsymbol{\gamma}_{\text{env}}$. The analysis can be carried out as in the single-DoF case. In detail, choosing $\boldsymbol{K}_D$ and $\boldsymbol{K}_P$ as diagonal positive semi-definite matrices, and $\boldsymbol{M}_d$ as a diagonal positive definite matrix ($\boldsymbol{M}_d$ must be invertible in view of (10.36)), this equation defines a passive impedance from the velocity $\dot{\boldsymbol{y}}$ to the generalized interaction force $-\boldsymbol{\gamma}_{\text{env}}$. Therefore, coupled stability is guaranteed in case of interaction with any passive environment.

Note that this ideal behavior can be obtained only in the hypothesis that friction torques are negligible, or they can be completely canceled by a suitable model-based compensation term to be added to the control torque (10.33), which is unlikely to happen. Also, although the dynamics of the controlled robot is independent of the robot configuration, if the control gains $\boldsymbol{M}_d$, $\boldsymbol{K}_D$, $\boldsymbol{K}_P$ are set to ensure good performance when the robot is in contact with the environment, they could not be adequate during free motion and vice versa.

Figure 10.8 illustrates a concept schematic of the overall system, with the impedance control, the robot–impedance and the environment–admittance. The dashed line is the (optional) force feedback used to modify the inertia of the robot projected in task space.

Admittance Control

Admittance control can be used only if the interaction force measure $\boldsymbol{\gamma}_{\text{env}}$ is available. The admittance control scheme of Fig. 10.6 can be easily generalized to multiple joint robots by employing a high-gain inner motion control loop to cope with friction and ensure tracking of a reference motion trajectory. This feedback control loop can also cancel out the joint torque produced by the interaction with the environment, by using the measurement of $\boldsymbol{\gamma}_{\text{env}}$.

To better understand the difference with respect to impedance control with force feedback, assume that inner motion control is of task-space feedback linearizing

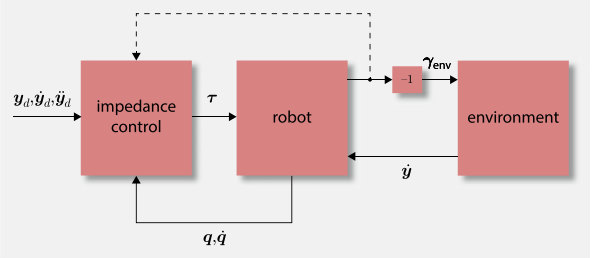

Fig. 10.8 Concept schematic of the robot–environment system with impedance control

type, i.e., based on (10.33) and (10.34). If the control input $\boldsymbol{a}_y$ in (10.34) is chosen as

$$\boldsymbol{a}_y = \ddot{\boldsymbol{y}}_c + \boldsymbol{K}_1 \dot{\boldsymbol{e}}_y + \boldsymbol{K}_2 \boldsymbol{e}_y, \tag{10.38}$$

where $\boldsymbol{y}_c(t)$ is a suitable task-space trajectory and $\boldsymbol{e}_y(t) = \boldsymbol{y}_c(t) - \boldsymbol{y}(t)$, the following equation is achieved for the error dynamics:

$$\ddot{\boldsymbol{e}}_y + \boldsymbol{K}_1 \boldsymbol{e}_y + \boldsymbol{K}_2 \boldsymbol{e}_y = \boldsymbol{0},$$

which guarantees exponential stability at the origin for all positive definite $\boldsymbol{K}_1$ and $\boldsymbol{K}_2$. The control gains $\boldsymbol{K}_1$ and $\boldsymbol{K}_2$ are set so as to achieve fast convergence of the tracking error (i.e., $\boldsymbol{y}(t) \approx \boldsymbol{y}_c(t)$) and good rejection of friction and other disturbance torques.

The task-space trajectory $\boldsymbol{y}_c(t)$ is computed as the output of an admittance equation, with the generalized interaction force $-\gamma_{\text{env}}$ as input i.e., integrating the differential equation

$$\boldsymbol{M}_d(\ddot{\boldsymbol{y}}_c - \ddot{\boldsymbol{y}}_d) + \boldsymbol{K}_D(\dot{\boldsymbol{y}}_c - \dot{\boldsymbol{y}}_d) + \boldsymbol{K}_P(\boldsymbol{y}_c - \boldsymbol{y}_d) = -\gamma_{\text{env}}, \tag{10.39}$$

with initial conditions $\dot{\boldsymbol{y}}_c(0) = \dot{\boldsymbol{y}}_d(0)$, $\boldsymbol{y}_c(0) = \boldsymbol{y}_d(0)$. The desired position $\boldsymbol{y}_d(t)$, velocity $\dot{\boldsymbol{y}}_d(t)$ and acceleration $\ddot{\boldsymbol{y}}_d(t)$ are feedforward inputs that can be set to zero to analyze passivity and coupled stability. Choosing $\boldsymbol{M}_d$, $\boldsymbol{K}_D$, $\boldsymbol{K}_P$ as diagonal matrices, the analysis is identical to that in the case of 1 DoF.

In the absence of interaction ($\gamma_{\text{env}} = \boldsymbol{0}$), the output of the admittance Eq. (10.39) is $\boldsymbol{y}_c(t) = \boldsymbol{y}_d(t)$, and thus the inner motion controller ensures the tracking of the desired trajectory $\boldsymbol{y}_d(t)$. In the presence of interaction ($\gamma_{\text{env}} \neq \boldsymbol{0}$), the solution $\boldsymbol{y}_c(t)$ to the admittance equation deviates from the desired trajectory $\boldsymbol{y}_d(t)$, which becomes a virtual trajectory. Thus, the inner motion control, while ensuring tracking of $\boldsymbol{y}_c(t)$, imposes to the robot a compliant behavior consistent with the interaction force γ_{env} and the admittance parameters.

From the above analysis, it is clear that the dynamics of motion control, which depends on the gain matrices $\boldsymbol{K}_1$, $\boldsymbol{K}_2$, is independent of the dynamics of the desired admittance, which can be tuned to the dynamics of the environment by setting the matrices $\boldsymbol{M}_d$, $\boldsymbol{K}_D$, $\boldsymbol{K}_P$. In fact, this is an advantage of admittance control. The drawback is that the outer admittance controller 'feels' the interaction force only

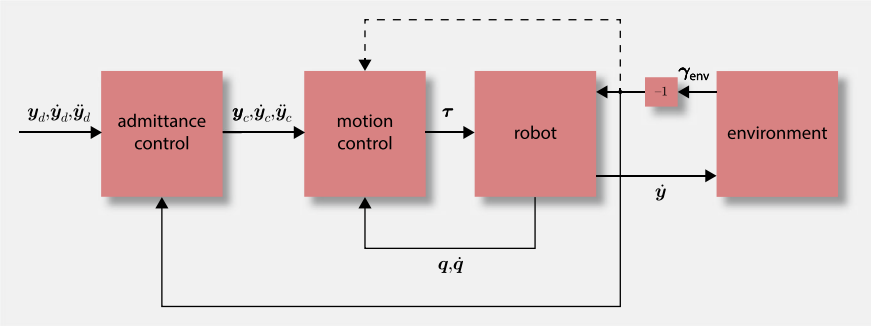

Fig. 10.9 Concept schematic of the robot–environment system with admittance control

through the force sensor. Therefore, if interaction occurs in a part of the robot body where the force is not measured or estimated, this latter is rejected as a disturbance by the inner motion controller. This may produce unsafe behavior, with large interaction forces, especially in the presence of unexpected obstacles or humans.

Figure 10.9 illustrates a concept schematic of the overall system, with the inner motion control, the outer admittance control, and the robot–admittance interacting with the environment–impedance. The dashed line represents the (optional) force feedback that can be used by the inner motion control.

Example 10.3 To gain a better insight into the difference between impedance and admittance control, consider the same task of Example 10.2.

Assume first that impedance control (10.33), (10.34), (10.36) is used, with scalar gain matrices $M_d = m_d \boldsymbol{I}$, $K_D = k_D \boldsymbol{I}$, and $\boldsymbol{K}_P = k_P \boldsymbol{I}$. Due to the simple geometry of the problem, Eq. (10.37) of the coupled system can be split into the two scalar differential equations:

$$m_d \ddot{x}_e + k_D \dot{x}_e + (k_P + k) x_e = k_P x_d + k x_r \tag{10.40}$$

$$m_d \ddot{z}_e + k_D \dot{z}_e + k_P z_e = k_P z_d. \tag{10.41}$$

Note that only the first equation, describing the horizontal motion, is influenced by the elastic force $k(x_e - x_r)$. At the equilibrium, the position and force are the same of compliant control in Example 10.2. Asymptotic stability of the equilibrium is guaranteed by using strictly positive gains. Since the two equations are linear and decoupled, it is easy to predict the effects of the choice of the control gains on the time response of the system. Both the equations are of second order. The damping ratio ζ and natural frequency ω_n for the equation of the horizontal motion are

$$\zeta = \frac{k_D}{2\sqrt{m_d (k_P + k)}} \qquad \omega_n = \sqrt{\frac{k_P + k}{m_d}}.$$

The same relationships hold for the equation of the vertical motion, by setting $k = 0$. Note that the above linear and decoupled equations are obtained assuming that joint friction is negligible or compensated. The higher the (noncompensated) friction, the higher the impedance gains and, in particular the stiffness k_P, so that the effects of friction can be neglected. Once k_P is selected, the gains m_d and k_D can be chosen with $\zeta \geq 1$ for the damping ratio in the first equation so as to avoid overshoot and oscillation of position and force during the transient. This can be achieved if an (upper bound) estimate of the stiffness k is available. In case that, as in this example, the same gains are used along the vertical direction, where the robot is free to move ($k = 0$), the motion control could result excessively overdamped and slow.

If admittance control (10.33), (10.34), (10.38), (10.39) is used, for the free motion along the vertical direction it is possible to assume $z_c = z_d$, because the input force in the admittance equation of the vertical coordinate is null and, at time $t = 0$, it is $z_c(0) = z_d(0)$. Therefore, the coordinate $z_e(t)$ of the robot position evolves according to the dynamics imposed by the motion controller

$$\ddot{z}_e + k_1 \dot{z}_e + k_2 z_e = k_2 z_d,$$

being $\boldsymbol{K}_1 = k_1 \boldsymbol{I}$, $\boldsymbol{K}_2 = k_2 \boldsymbol{I}$ in (10.39). These motion control gains can be chosen so as to guarantee good tracking and disturbance rejection capability. On the other hand, the desired position along the horizontal direction, together with the contact force, generates the position reference $x_c(t)$, which is input to the inner motion controller, together with the feedforward of velocity $\dot{x}_c(t)$ and acceleration $\ddot{x}_c(t)$. Since the bandwidth of the inner motion control loop is usually much larger that that of the desired admittance, it is reasonable to assume $x_e(t) \approx x_c(t)$. Thus, the differential equation of the position coordinate $x_e(t)$ is the same as in (10.40). The difference is that with admittance control the gains m_d, k_D and k_P can be set only on the basis of the desired compliant behavior for a given estimate k of the stiffness coefficient, and do not affect the motion tracking and disturbance rejection capability, which depend on k_1 and k_2. ■

6-DoF Tasks

The selection of good impedance parameters, in order to achieve satisfactory behavior during the interaction, is not an easy task. Examples 10.2 and 10.3 showed that the closed-loop dynamics along the free motion directions is different from that along the directions where interaction occurs. Moreover, in the latter case, the transient behavior and the value of the interaction force depend both on the robot and the environment dynamics. Therefore, the execution of a complex task, involving different types of interaction, may require different values of the impedance parameters along different task directions.

Often the task concerns the end-effector of a robot manipulator and involves the end-effector position and orientation, together with the interaction wrench, i.e., the force and moment exchanged at the interaction. For the analysis of these 6-DoF tasks, at least in static conditions, a suitable model of the elastic-type interaction wrench is required.

A 6-DoF elastic model can be defined by considering two elastically coupled rigid bodies, $\mathcal{A}$ and $\mathcal{B}$, and two reference frames, O_a–$x_a y_a z_a$ and O_b–$x_b y_b z_b$, each attached to one of the two bodies so that at equilibrium, in the absence of forces and moments, the two frames coincide. Let $\Delta \boldsymbol{t}_{ba}$ denote an elementary displacement from the equilibrium of frame b with respect to frame a, defined as

$$\Delta \boldsymbol{t}_{ab} = (\boldsymbol{t}_b - \boldsymbol{t}_a)dt, \tag{10.42}$$

being $\boldsymbol{t}_a = (\boldsymbol{v}_a, \boldsymbol{\omega}_a)$ and $\boldsymbol{t}_b = (\boldsymbol{v}_b, \boldsymbol{\omega}_b)$ the twists of frame a and frame b, respectively. This elementary displacement can be equivalently referred to as frame a or b because, at equilibrium, the two frames coincide and the deformation is small. To the displacement $\Delta \boldsymbol{t}_{ab}$, coinciding with the deformation of the spring between the bodies $\mathcal{B}$ and $\mathcal{A}$, corresponds the elastic wrench

$$\boldsymbol{w}_{\text{el}} = \begin{pmatrix} \boldsymbol{f}_{\text{el}} \\ \boldsymbol{\mu}_{\text{el}} \end{pmatrix} = - \begin{pmatrix} \boldsymbol{K}_t & \boldsymbol{K}_c \\ \boldsymbol{K}_c^T & \boldsymbol{K}_o \end{pmatrix} \Delta \boldsymbol{t}_{ab} = - \boldsymbol{K} \Delta \boldsymbol{t}_{ab}. \tag{10.43}$$

In view of the action–reaction law, the wrench $\boldsymbol{w}_b$ applied by body $\mathcal{B}$ on the spring is opposite to the elastic wrench, i.e., $\boldsymbol{w}_b = - \boldsymbol{w}_{\text{el}} = \boldsymbol{K} \Delta \boldsymbol{t}_{ab}$, while the wrench $\boldsymbol{w}_a$ applied by body $\mathcal{A}$ is $\boldsymbol{w}_a = - \boldsymbol{w}_b = \boldsymbol{K} \Delta \boldsymbol{t}_{ba}$, being $\Delta \boldsymbol{t}_{ba} = - \Delta \boldsymbol{t}_{ab}$. All these quantities can be equivalently referred to one of the two reference frames.

The 6×6 matrix $\boldsymbol{K}$ is a *stiffness matrix*, which is symmetric and *positive semi-definite*. The 3×3 matrices $\boldsymbol{K}_t$ and $\boldsymbol{K}_o$ are known as *translational stiffness* and *rotational stiffness*, respectively. The 3×3 matrix $\boldsymbol{K}_c$ is known as *coupling stiffness*. An analogous decomposition can be made for the *compliance matrix* $\boldsymbol{C}$ in the mapping

$$\Delta \boldsymbol{t}_{ab} = - \boldsymbol{C} \boldsymbol{w}_{\text{el}}. \tag{10.44}$$

In real elastic systems, matrix $\boldsymbol{K}_c$ is, in general, nonsymmetric. However, there are special devices such as the RCC, where $\boldsymbol{K}_c$ can be symmetric or null. These are elastically compliant mechanical devices, suitably designed to achieve maximum decoupling between translation and rotation of a frame located in a point in space denoted by RCC. These devices are interposed between the manipulator last link and the end-effector, with the aim of introducing a *passive compliance* to facilitate the execution of assembly tasks. An example of a RCC device used to facilitate peg-in-hole insertion is illustrated in Fig. 10.10. The RCC frame is located near the tip of the peg. If the peg is perfectly aligned and centered to the hole, it would slide inside when the robot gripper moves vertically. However, if, as in the figure, the peg's alignment or centering is slightly off, the peg contacts one side of the hole first, and the peg's tip experiences a lateral force, which, thanks to the translational compliance of the device, allows the center of compliance to shift laterally toward the center of the hole, so that the peg starts sliding in the hole. When, due to the misalignment of the peg and hole axes, the tip experiences a second contact with the opposite side of the hole, the resulting moment produces a rotation of the RCC device about the center of compliance which reduces the misalignment and facilitates the insertion.

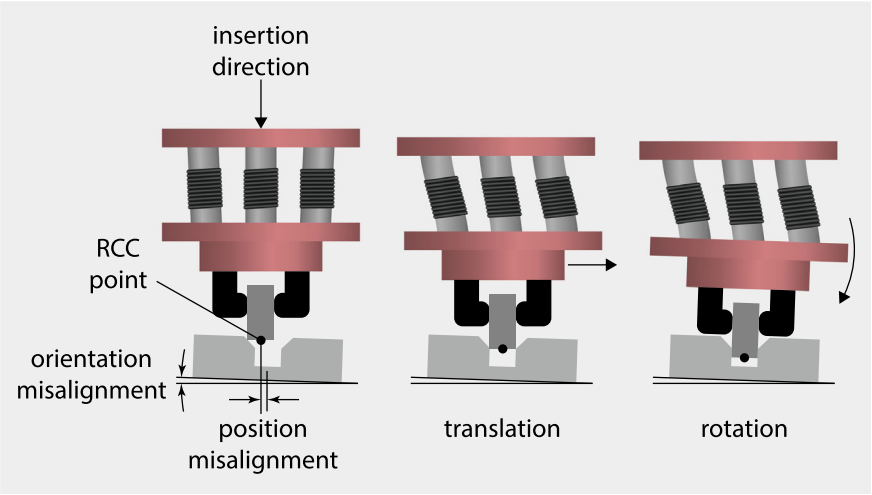

Fig. 10.10 Example of RCC device used for peg-in-hole insertion

The inconvenience of such devices is their low versatility for different operating conditions and generic interaction tasks, which may require the modification of the compliant mechanical hardware. On the other hand, considering the closed-loop equations of compliance control (10.26), (10.28), impedance control (10.31), (10.37), or admittance control (10.39), the following equality holds at steady-state:

$$\gamma_{\text{env}} = \boldsymbol{K}_P \boldsymbol{e}_{\boldsymbol{y}} = -\boldsymbol{K}_P(\boldsymbol{y}_e - \boldsymbol{y}_d). \tag{10.45}$$

If the task vector is the end-effector pose, i.e., $\boldsymbol{y} = \boldsymbol{y}_e$, the above equation shows that, at steady state, the end-effector behaves like a spring of stiffness $\boldsymbol{K}_P$ in task coordinates, which produces an elastic force γ_{env} in response to a displacement $\boldsymbol{y}_e - \boldsymbol{y}_d$ from the equilibrium pose $\boldsymbol{y}_d$. This behavior corresponds, in essence, to an *active compliance* (or, equivalently, an active stiffness) that can be easily modified by acting on the gain matrix $\boldsymbol{K}_P^{-1}$ so as to satisfy the requirements of different interaction tasks.

For the selection of the parameters of a 6-DoF active stiffness according the task geometry, it is useful to derive an elastic model of the form (10.43) from mapping (10.45), with a suitable choice of the end-effector pose error. For simplicity, assume that $\boldsymbol{K}_P$ is block diagonal, i.e., $\boldsymbol{K}_P = \text{diag}\{\boldsymbol{K}_{Pt}, \boldsymbol{K}_{Po}\}$ with 3×3 symmetric and positive definite matrices $\boldsymbol{K}_{Pt}$ and $\boldsymbol{K}_{Po}$.

The relative pose of the desired frame O_d–$x_d y_d z_d$ of position $\boldsymbol{p}_d$ and orientation $\boldsymbol{R}_d$, with respect to the end-effector frame O_e–$x_e y_e z_e$ of position $\boldsymbol{p}_e$ and orientation $\boldsymbol{R}_e$ can be expressed using the task error

$$\boldsymbol{e}_{\boldsymbol{y}} = \begin{pmatrix} \boldsymbol{e}_p \\ \boldsymbol{e}_o \end{pmatrix} = \begin{pmatrix} \boldsymbol{p}_d - \boldsymbol{p}_e \\ \boldsymbol{\phi}_{ed} \end{pmatrix}. \tag{10.46}$$

The orientation error $\boldsymbol{e}_o = \boldsymbol{\phi}_{ed}$ is the triplet of XYZ Euler angles extracted from ${}^e\boldsymbol{R}_d = \boldsymbol{R}_e^T \boldsymbol{R}_d$. The XYZ angles are preferred to other triplets of Euler angles because the differential mapping

$$\dot{\boldsymbol{e}}_o = \boldsymbol{T}_E^{-1}(\boldsymbol{\phi}_{ed})\,(\boldsymbol{\omega}_d - \boldsymbol{\omega}_e) \tag{10.47}$$

computed in (3.122) is not singular for $\boldsymbol{\phi}_{ed} = \boldsymbol{0}$ and, also, $\boldsymbol{T}_E(\boldsymbol{0}) = \boldsymbol{R}_e\,{}^e\boldsymbol{T}_E(\boldsymbol{0}) = \boldsymbol{R}_e$. In view of (10.47), the following equality holds:

$$\dot{\boldsymbol{e}}_y = \begin{pmatrix} \boldsymbol{I} & \boldsymbol{O} \\ \boldsymbol{O} & \boldsymbol{T}_E^{-T}(\boldsymbol{\phi}_{ed}) \end{pmatrix} (\boldsymbol{t}_d - \boldsymbol{t}_e),$$

and the elementary displacement in task coordinates about the equilibrium $\boldsymbol{e}_y = \boldsymbol{0}$ is

$$d\boldsymbol{e}_y = \dot{\boldsymbol{e}}_y\Big|_{\boldsymbol{e}_y=\boldsymbol{0}} dt = \begin{pmatrix} \boldsymbol{R}_e & \boldsymbol{O} \\ \boldsymbol{O} & \boldsymbol{I} \end{pmatrix} \Delta\boldsymbol{t}_{ed}, \tag{10.48}$$

being $\Delta\boldsymbol{t}_{ed} = ({}^e\boldsymbol{t}_d - {}^e\boldsymbol{t}_e)dt$. On the other hand, the application of the principle of virtual work leads to the corresponding transformation among wrench and generalized force at the equilibrium:

$${}^e\boldsymbol{w}_{\text{env}} = \begin{pmatrix} \boldsymbol{R}_e^T & \boldsymbol{O} \\ \boldsymbol{O} & \boldsymbol{I} \end{pmatrix} \boldsymbol{\gamma}_{\text{env}}. \tag{10.49}$$

Plugging (10.45) into (10.49), with $d\boldsymbol{e}_y$ in (10.48) in place of $\boldsymbol{e}_y$, yields

$${}^e\boldsymbol{w}_{\text{env}} = \boldsymbol{K}_A \Delta\boldsymbol{t}_{ed}, \tag{10.50}$$

where $\boldsymbol{K}_A = \text{diag}\{\boldsymbol{R}_e^T \boldsymbol{K}_{Pt} \boldsymbol{R}_e, \boldsymbol{K}_{Po}\}$ is the active stiffness related to the elastic behaviour of the controlled robot about the equilibrium $\boldsymbol{e}_y = \boldsymbol{0}$.[5]

For the selection of the elements of $\boldsymbol{K}_A$, assume that the interaction force between the end-effector and the environment derives from a generalized spring acting between the end-effector frame O_e–$x_e y_e z_e$ and a rest frame O_r–$x_r y_r z_r$ attached to the environment rest position. Considering an elementary displacement $\Delta\boldsymbol{t}_{re}$ between the two reference frames, the corresponding wrench applied by the end-effector is

$${}^e\boldsymbol{w}_{\text{env}} = \boldsymbol{K}\Delta\boldsymbol{t}_{re} \tag{10.51}$$

with a stiffness matrix $\boldsymbol{K}$. Typically, the stiffness matrix is positive semi-definite because, in general, the interaction forces and moments belong to some particular directions, spanning $\mathcal{R}(\boldsymbol{K})$.

Using (10.50), (10.51) and the equality $\Delta\boldsymbol{t}_{re} = \Delta\boldsymbol{t}_{rd} - \Delta\boldsymbol{t}_{ed}$, the following expression can be found (see Problem 10.7):

$${}^e\boldsymbol{w}_{\text{env}} = \left(\boldsymbol{I}_6 + \boldsymbol{K}\boldsymbol{K}_A^{-1}\right)^{-1} \boldsymbol{K}\Delta\boldsymbol{t}_{rd}. \tag{10.52}$$

[5] Other definitions of orientation error, e.g., based on axis–angle or unit quaternion, can be adopted, leading to (10.50).

Plugging (10.52) into the inverse of Eq. (10.50) yields

$$\Delta \boldsymbol{t}_{ed} = \boldsymbol{K}_A^{-1}\left(\boldsymbol{I}_6 + \boldsymbol{K}\boldsymbol{K}_A^{-1}\right)^{-1}\boldsymbol{K}\Delta \boldsymbol{t}_{rd}, \tag{10.53}$$

representing the pose error of the end-effector at the equilibrium. Note that vectors in (10.52) and (10.53) can be referred, equivalently, to the end-effector frame, to the desired frame or to the rest frame; all these frames coincide at equilibrium.

The analysis of (10.53) shows that the end-effector pose error at equilibrium depends on the rest position of the environment, as well as the desired pose imposed by the manipulator control system. The interaction of the two systems (environment and manipulator) is influenced by the mutual weight of the respective compliance features.

In fact, it is possible to modify active compliance $\boldsymbol{K}_A^{-1}$ so that the manipulator dominates the environment and vice versa. This dominance can be specified with reference to the single directions of the task space.

Assume that, for simplicity, both $\boldsymbol{K}$ and $\boldsymbol{K}_A$ are diagonal, so there is a decoupled behavior along the task directions. For a given stiffness of the environment $\boldsymbol{K}$, according to the prescribed interaction task, one can choose large values of the elements of $\boldsymbol{K}_A$ for the directions along which the environment has to comply and small values of the elements of $\boldsymbol{K}_A$ for those directions along which the manipulator has to comply. As a consequence, the manipulator pose error $\Delta \boldsymbol{t}_{ed}$ tends to zero along the directions where the environment complies; vice versa, along the directions where the manipulator complies, the end-effector pose tends to the rest pose of the environment, namely $\Delta \boldsymbol{t}_{ed} \approx \Delta \boldsymbol{t}_{rd}$.

Equation (10.52) gives the value of the contact wrench at the equilibrium. This expression reveals that, along the directions where the stiffness of the manipulator is much higher than the stiffness of the environment, the intensity of the elastic wrench depends mainly on the stiffness of the environment and on the displacement $\Delta \boldsymbol{t}_{re}$ between the equilibrium pose of the end-effector (close the desired pose) and the rest pose of the environment. In the dual case that the stiffness of the environment is much higher than the stiffness of the manipulator, the intensity of the elastic wrench depends mainly on the stiffness of the manipulator and the displacement $\Delta \boldsymbol{t}_{ed}$ between the desired pose and the equilibrium pose of the end-effector (close to the rest pose of the environment).

10.3 Constrained Motion

Impedance control ensures stability of the coupled robot–environment system without requiring a model of the environment, provided that both the controlled robot and the environment are passive. However, there are situations where specifying the dynamic relationship between force and motion is not enough and the successful execution of the task requires the capability of controlling both the end-effector motion and the interaction force along different directions.

A typical example is that of a robot manipulator cleaning a glass window. In this case, the manipulator should be controlled so that the cleaning tool moves on the glass surface while keeping contact and applying a suitable force.

This kind of contact situation can be modeled by making simplifying assumptions, namely:

- both the robot and the environment are rigid and pure geometric constraints are imposed by the environment at the contact;
- the robot is rigid and the interaction produces a local deformation of the environment which is approximated by a linear elastic model.

In the former, reaction forces and moments arise when the robot tends to violate the constraints. In the latter, the reaction wrench is proportional to the component of robot's displacement corresponding to environment's local deformation. In both cases, frictionless contact is assumed. It is obvious that the above assumptions are only ideal. However, the robustness of the controller should be able to cope with situations where some of the assumptions are not fully satisfied.

For the sake of clarity, the case of interaction on the end-effector of a n-DoFs manipulator, with $n \geq 6$, is considered. The velocity of the end-effector frame is described by a 6-dimensional twist vector $\boldsymbol{t}_e$. The forces and moments applied by the robot to the environment on a contact point or through a contact surface, are described by a 6-dimensional wrench vector $\boldsymbol{w}_{\text{env}}$.

The geometric constraints imposed by the environment on the motion of the robot's end-effector reduce the dimension of the space of the feasible end-effector twists and wrenches.

In the presence of k independent constraints ($k < 6$), the end-effector twist belongs to a subspace of dimension $6-k$, hereafter denoted as *twist control subspace*, while the end-effector wrench belongs to a subspace of dimension k, hereafter denoted as *wrench control subspace*, and can be expressed in the form

$$\boldsymbol{t}_e = \boldsymbol{S}_t(\boldsymbol{q})\boldsymbol{\nu} \qquad \boldsymbol{w}_{\text{env}} = \boldsymbol{S}_w(\boldsymbol{q})\boldsymbol{\lambda}_{\text{env}}, \tag{10.54}$$

where $\boldsymbol{\nu}$ is the $(6-k)$-dimensional vector of the twist components along the columns of $\boldsymbol{S}_t(\boldsymbol{q})$ and $\boldsymbol{\lambda}_{\text{env}}$ is the k-dimensional vector of the wrench components along the columns of $\boldsymbol{S}_w(\boldsymbol{q})$. Matrices $\boldsymbol{S}_t$ and $\boldsymbol{S}_w$ are known as *selection matrices*. In general, they depend on the end-effector pose variables $\boldsymbol{y}_e$ and thus, from direct kinematics (2.55), on generalized coordinates $\boldsymbol{q}$.

Note that, while subspace $\mathcal{R}(\boldsymbol{S}_t)$ and $\mathcal{R}(\boldsymbol{S}_w)$ are uniquely defined by the geometry of the contact, matrices $\boldsymbol{S}_t$ and $\boldsymbol{S}_w$ are not uniquely defined. Whenever possible, it is convenient to choose $\boldsymbol{S}_t$ so that its columns are a set of $6-k$ linearly independent twists and $\boldsymbol{S}_w$ so that its columns are a set of k linearly independent wrenches. In this way $\boldsymbol{\nu}$ and $\boldsymbol{\lambda}_{\text{env}}$ are dimensionless vectors. This choice guarantees that, in the case of a change in the reference frame or measurement units, the transformations to be applied to matrices $\boldsymbol{S}_t$ and $\boldsymbol{S}_w$ are well defined on the basis of their physical meaning.

The wrench and twist control subspaces are *reciprocal*, i.e.,

$$\boldsymbol{w}_{\text{env}}^T \boldsymbol{t}_e = 0 \qquad \boldsymbol{S}_w^T(\boldsymbol{q}) \boldsymbol{S}_t(\boldsymbol{q}) = \boldsymbol{O}. \tag{10.55}$$

The concept of reciprocity expresses the physical fact that, in the hypothesis of rigid and frictionless contact, the wrench does not cause any work against the twist. This concept is often confused with the concept of orthogonality, which is meaningless in this case because twists and wrenches are nonhomogeneous quantities that belong to different vector spaces. In view of the assumptions made for compliant contact, reciprocity also holds in this case.

In case of compliant contact, along some directions both motion and force are allowed, although they are not independent. In view of the assumption of small local deformation of elastic type of the environment, it is convenient to include such directions in the wrench control subspace. Since the contact can be compliant along some directions and rigid along some other directions, the wrench control subspace can be decomposed into two distinct subspaces, one corresponding to the reaction forces to the rigid contact and the other corresponding to the elastic forces, which depend on the deformation.

An interaction task can be assigned in terms of desired end-effector twist $\boldsymbol{t}_d$ and wrench $\boldsymbol{w}_d$ that are computed as

$$\boldsymbol{t}_d = \boldsymbol{S}_t(\boldsymbol{q}) \boldsymbol{\nu}_d \qquad \boldsymbol{w}_d = \boldsymbol{S}_w(\boldsymbol{q}) \boldsymbol{\lambda}_d, \tag{10.56}$$

by specifying $\boldsymbol{\nu}_d$ and $\boldsymbol{\lambda}_d$. Vice versa, these quantities can be computed as

$$\boldsymbol{\nu}_d = \boldsymbol{S}_t^{\dagger}(\boldsymbol{q}) \boldsymbol{t}_d \qquad \boldsymbol{\lambda}_d = \boldsymbol{S}_w^{\dagger}(\boldsymbol{q}) \boldsymbol{w}_d, \tag{10.57}$$

by specifying $\boldsymbol{w}_d$ and $\boldsymbol{t}_d$, where $\boldsymbol{S}_t^{\dagger}$ and $\boldsymbol{S}_w^{\dagger}$ are pseudoinverses of $\boldsymbol{S}_t$ and $\boldsymbol{S}_w$ respectively.[6]

The computation of $\boldsymbol{S}_t$ and $\boldsymbol{S}_w$ can be performed using a geometric approach or an analytic approach.

10.3.1 Geometric Approach

In many robotic tasks it is possible to set an orthogonal reference frame, usually referred as *task frame*, in which the matrices $\boldsymbol{S}_t$ and $\boldsymbol{S}_w$ are constant. The task frame can be chosen either attached to the end-effector or to the environment. Moreover, the interaction task is specified by assigning a desired force/torque or a desired linear/angular velocity along/about each of the frame axes. The following can be observed.

[6] See Appendix A.7 for the definition of pseudoinverse.

- Along/about each axis, the environment imposes to the manipulator's end-effector either a velocity constraint—in the sense that it does not allow translation along a direction or rotation about an axis—or a force constraint—in the sense that it does not allow the application of any force along a direction or any torque about an axis; such constraints are called *natural constraints* since they are determined directly by task geometry.
- The manipulator can control only the variables that are not subject to natural constraints; the reference values for these variables are called *artificial constraints* since they are imposed with regard to the strategy to perform the given task.

Note that the two sets of constraints are complementary in that they regard different variables for each axis. Also, they allow a complete specification of the task, since they involve all variables.

In the case of compliant environment, for each axis along/about which the interaction occurs, in principle one can choose the variable to control, namely the force or velocity, as long as the complementarity of the constraint is preserved. However, in view of the assumption on the type of interaction made above, the force is chosen as an artificial constraint and the velocity as a natural constraint, as for the case of a rigid environment.

To illustrate the description of an interaction task in terms of natural and artificial constraints as well as to emphasize the opportunity to use a task frame for task specification, in the following a number of typical case studies are analyzed.

Sliding on a planar surface—The task is the sliding of a prismatic object on a planar surface while pushing with a given force. Task geometry suggests choosing the task frame as attached to the contact plane with an axis orthogonal to the plane (Fig. 10.11). Alternatively, the task frame can be chosen with the same orientation but attached to the object.

Natural constraints can be determined first, assuming rigid and frictionless contact. Velocity constraints describe the impossibility to generate a linear velocity along axis z_t and angular velocities along axes x_t and y_t. Force constraints describe the impossibility to exert forces along axes x_t and y_t and a moment along axis z_t.

The artificial constraints regard the variables not subject to natural constraints. Hence, in view of the complementarity, it is possible to specify artificial constraints for force along z_t, moments about x_t and y_t, linear velocity along axis z_t and angular velocity about axes x_t and y_t. The constraints are summarized in Table 10.1, where bullets indicate the variables subject to natural or artificial constraints.

For this task, the dimension of the wrench control subspace is $k = 3$, while the dimension of the twist control subspace is $6-h = 3$. Let $\boldsymbol{e}_i$ denote the i-th column of the 6×6 identity matrix, representing both a unit twist and a unit wrench. Matrices $\boldsymbol{S}_t$ and $\boldsymbol{S}_w$ can be chosen as

$$\boldsymbol{S}_t = \begin{pmatrix} \boldsymbol{e}_1 & \boldsymbol{e}_2 & \boldsymbol{e}_6 \end{pmatrix} \qquad \boldsymbol{S}_w = \begin{pmatrix} \boldsymbol{e}_3 & \boldsymbol{e}_4 & \boldsymbol{e}_5 \end{pmatrix}.$$

Note that, if the task frame is chosen attached to the contact plane, matrices $\boldsymbol{S}_t$ and $\boldsymbol{S}_w$ remain constant if referred to the base frame but are time-varying if referred to

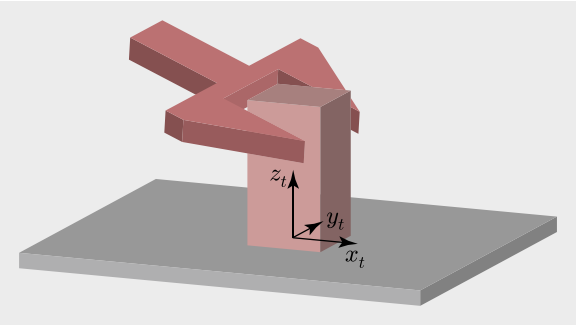

Fig. 10.11 Sliding of a prismatic object on a planar surface

Table 10.1 Variables subject to natural and artificial constraints for the task of sliding on a planar surface

	v_x	v_y	v_z	w_x	w_y	w_z	f_x	f_y	f_z	m_x	m_y	m_z
Natural			•	•	•		•	•				•
Artificial	•	•				•			•	•	•	

the end-effector frame. Vice versa, if the task frame is chosen attached to the object, such matrices are constant if referred to the end-effector frame and time-varying if referred to the base frame.

If the plane is elastically compliant in the vertical direction, i.e., the forces along axis z_t are of elastic type, then the wrench control subspace can be split into two subspaces, generated by the columns of matrices

$$\boldsymbol{S}'_w = \boldsymbol{e}_3 \qquad \boldsymbol{S}''_w = \begin{pmatrix} \boldsymbol{e}_4 & \boldsymbol{e}_5 \end{pmatrix}$$

with obvious meaning of $\boldsymbol{S}'_w$ and $\boldsymbol{S}''_w$. Assuming the task frame attached to the contact plane in the undeformed configuration, the elastic wrench can be computed as $\boldsymbol{w}_{\text{env}} = \boldsymbol{K}\,\Delta\boldsymbol{t}_{te}$, being $\Delta\boldsymbol{t}_{te}$ the elementary displacement of the end-effector frame with respect to task frame and $\boldsymbol{K}$ the stiffness matrix. This latter can be defined as

$$\boldsymbol{K} = k_{33}\boldsymbol{e}_3\boldsymbol{e}_3^T,$$

where k_{33} is the stiffness coefficient of the plane along the vertical direction. The compliance relationship is $\Delta\boldsymbol{t}_{te} = \boldsymbol{C}\boldsymbol{w}_{\text{env}}$, with

$$\boldsymbol{C} = c_{33}\boldsymbol{e}_3\boldsymbol{e}_3^T,$$

and $c_{33} = k_{33}^{-1}$. Note that both $\boldsymbol{K}$ and $\boldsymbol{C}$ are positive semi-definite matrices with a positive constant in the (3, 3) entry and 0 in all the others.

If the contact plane is compliant also about axes x_t and y_t, then $\boldsymbol{S}_{we} = \boldsymbol{S}_w$. In this case, the definitions of the stiffness and compliance matrices involve multiple directions and the computation of these matrices can be made by generalizing the result for the single direction. In the simplifying assumption of complete decoupling

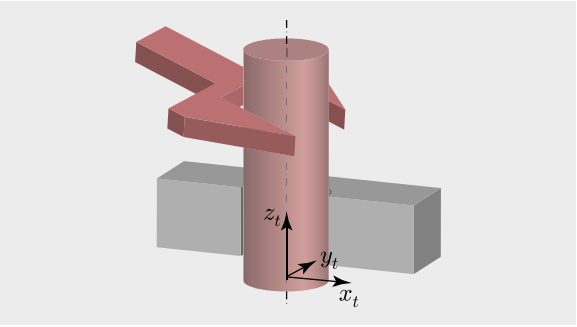

Fig. 10.12 Insertion of a cylindrical peg in a hole

Table 10.2 Variables subject to natural and artificial constraints for the peg-in-hole task

	v_x	v_y	v_z	w_x	w_y	w_z	f_x	f_y	f_z	m_x	m_y	m_z
Natural	•	•		•	•				•			•
Artificial			•			•	•	•		•	•	

of the elastic behavior along and about the axes of the task frame, it is

$$\boldsymbol{K} = \sum_{i=3}^{5} k_{ii} \boldsymbol{e}_i \boldsymbol{e}_i^T \qquad \boldsymbol{C} = \sum_{i=3}^{5} c_{ii} \boldsymbol{e}_i \boldsymbol{e}_i^T ,$$

with $c_{ii} = k_{ii}^{-1}$.

Peg-in-hole—The end-effector manipulation task is the insertion of a cylindrical object (peg) in a hole. Task geometry suggests choosing the task frame with the origin in the center of the hole and an axis parallel to the hole axis (Fig. 10.12). This frame can be chosen attached either to the peg or to the hole.

The natural constraints are determined by observing that it is not possible to generate arbitrary linear and angular velocities along axes x_t, y_t, nor is it possible to exert arbitrary force and moment along z_t. As a consequence, the artificial constraints can be used to specify forces and moments along x_t and y_t, as well as linear and angular velocity along z_t. The constraints are summarized in Table 10.2, where bullets indicate the variables subject to natural or artificial constraints.

Among the variables subject to artificial constraints, $v_z \neq 0$ describes insertion while the others are typically null. The task continues until a 'large' reaction force on the z_t direction is measured, indicating that the insertion is completed.

For this task, the dimension of the wrench control subspace is $k = 4$, while the dimension of the twist control subspace is $6 - k = 2$. Moreover, matrices $\boldsymbol{S}_t$ and $\boldsymbol{S}_w$ can be expressed as

$$\boldsymbol{S}_t = \begin{pmatrix} \boldsymbol{e}_3 & \boldsymbol{e}_6 \end{pmatrix} \qquad \boldsymbol{S}_w = \begin{pmatrix} \boldsymbol{e}_1 & \boldsymbol{e}_2 & \boldsymbol{e}_4 & \boldsymbol{e}_5 \end{pmatrix}$$

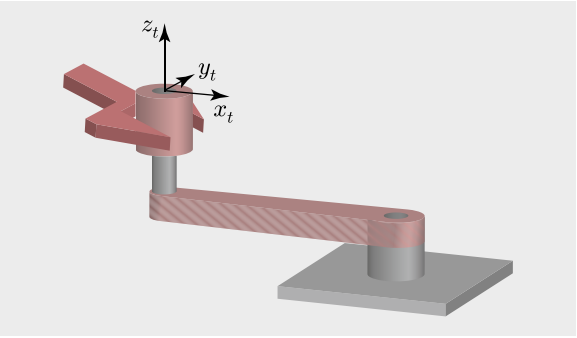

Fig. 10.13 Turning a crank

Table 10.3 Variables subject to natural and artificial constraints for the task of turning a crank

	v_x	v_y	v_z	w_x	w_y	w_z	f_x	f_y	f_z	m_x	m_y	m_z
Natural	•		•	•	•			•				•
Artificial		•				•	•		•	•	•	

Note that, if the task frame is chosen attached to the hole, matrices $\boldsymbol{S}_t$ and $\boldsymbol{S}_w$ remain constant if referred to the base frame but are time-varying if referred to the end-effector frame. Vice versa, if the task frame is chosen attached to the peg, such matrices are constant if referred to the end-effector frame and time-varying if referred to the base frame.

Turning a crank—The end-effector manipulation task is the turning of a crank. Task geometry suggests choosing the task frame with an axis aligned with the axis of the idle handle and another axis aligned with the crank lever (Fig. 10.13). Note that in this case the task frame is time-varying.

The natural constraints do not allow the generation of arbitrary linear velocities along x_t, z_t and angular velocities along x_t, y_t, nor arbitrary force along y_t and moment along z_t. As a consequence, the artificial constraints allow the specification of forces along x_t, z_t and moments along x_t, y_t, as well as a linear velocity along y_t and an angular velocity along z_t. The constraints are summarized in Table 10.3, where bullets indicate the variables subject to natural or artificial constraints.

Among the variables subject to artificial constraints, forces and moments are typically null for task execution.

For this task, the dimension of the wrench control subspace is $k = 4$, while the dimension of the twist control subspace is $6 - k = 2$. Moreover, matrices $\boldsymbol{S}_t$ and $\boldsymbol{S}_w$ can be expressed as

$$\boldsymbol{S}_t = \begin{pmatrix} \boldsymbol{e}_2 & \boldsymbol{e}_6 \end{pmatrix} \qquad \boldsymbol{S}_w = \begin{pmatrix} \boldsymbol{e}_1 & \boldsymbol{e}_3 & \boldsymbol{e}_4 & \boldsymbol{e}_5 \end{pmatrix}.$$

These matrices are constant in the task frame but are time-varying if referred to the base frame or to the end-effector frame, because the task frame moves with respect to both these frames during task execution.

10.3.2 Analytic Approach

The geometric constraints imposed by the environment to the robot end-effector, assumed both perfectly rigid, can be represented as a set of $k < 6$ algebraic equations that the variables describing the end-effector position and orientation must satisfy; since these variables depend on the joint variables through the direct kinematic equations, according to the analysis on constrained dynamics carried out in Sect. 5.10, the constraint equations can also be expressed in joint space as

$$\boldsymbol{h}(\boldsymbol{q}) = \boldsymbol{0}. \tag{10.58}$$

The constraints of the form (10.58) are *bilateral constraints*, because the reaction forces act so that, during the motion, the end-effector always keeps contact with the environment, as for the case of a gripper turning a crank. However, in many applications, the interaction with the environment corresponds to *unilateral constraints*. For instance, in the case of a tool sliding on a surface, the reaction forces/torques arise only when the tool pushes against the surface and not when it tends to detach. In the following analysis, Eq. (10.58) is considered to always be satisfied under the assumption that the end-effector, during the motion, never loses contact with the environment.

Using the EL formalism of Sect. 5.10, in the absence of joint friction and of friction at the contact, the following set of equations is obtained:

$$\boldsymbol{M}(\boldsymbol{q})\ddot{\boldsymbol{q}} + \boldsymbol{n}(\boldsymbol{q}, \dot{\boldsymbol{q}}) = \boldsymbol{\tau} + \boldsymbol{A}^T(\boldsymbol{q})\boldsymbol{\lambda}, \tag{10.59}$$

where $\boldsymbol{A}$ is the Jacobian matrix of the constraints $\boldsymbol{A}(\boldsymbol{q}) = \partial \boldsymbol{h}/\partial \boldsymbol{q}$ and $\boldsymbol{\lambda}$ is the k-dimensional vector of Lagrange multipliers. Vector $\boldsymbol{A}^T(\boldsymbol{q})\boldsymbol{\lambda}$ is the reaction joint torque corresponding to the reaction forces/torques at the end-effector due to the presence of the constraints.

In view of the results on the task-space dynamics of Sect. 5.9, the above equations for nonredundant robots can be rewritten in the form

$$\boldsymbol{\Lambda}_g(\boldsymbol{q})\dot{\boldsymbol{t}}_e + \boldsymbol{\Gamma}_g(\boldsymbol{q}, \dot{\boldsymbol{q}})\boldsymbol{t}_e + \boldsymbol{\eta}_g(\boldsymbol{q}) = \boldsymbol{w}_e - \boldsymbol{S}_w(\boldsymbol{q})\boldsymbol{\lambda}_{\text{env}}, \tag{10.60}$$

where $\boldsymbol{w}_e$ is the *control wrench* reflected at the end-effector, $\boldsymbol{\lambda}_{\text{env}} = -\boldsymbol{\lambda}$ is the vector of the constraint forces applied by the robot to the environment, and

$$\boldsymbol{S}_w(\boldsymbol{q}) = \boldsymbol{J}_M^{\dagger T}(\boldsymbol{q})\boldsymbol{A}^T(\boldsymbol{q}) \tag{10.61}$$

is an analytic expression of the $6 \times k$ selection matrix spanning the wrench control subspace. Note that matrix (10.61) is not uniquely defined, because function $\boldsymbol{h}(\boldsymbol{q})$ is not unique.

The selection matrix $\boldsymbol{S}_t(\boldsymbol{q})$ whose columns span the twist control subspace can be chosen as a matrix $6 \times (6 - k)$ that satisfies the reciprocity condition (10.55). In addition, this matrix is not uniquely defined.

An analytic form of $\boldsymbol{S}_t(\boldsymbol{q})$ can be found using the results of Sect. 5.10, assuming, for simplicity, $n = 6$. According to (5.157), the joint velocities that satisfy the

constraints (10.58) can be computed as

$$\dot{\boldsymbol{q}} = \boldsymbol{G}(\boldsymbol{q})\boldsymbol{\nu} \tag{10.62}$$

where $\boldsymbol{\nu}$ is a $(6-k)$-dimensional vector of reduced velocities and $\boldsymbol{G}(\boldsymbol{q})$ is the $6 \times (6-k)$ matrix computed in (5.156), with $\boldsymbol{A}\boldsymbol{G} = \boldsymbol{O}$. Therefore, the end-effector twists that satisfy the constraints (10.58) are given by

$$\boldsymbol{t}_e = \boldsymbol{J}_g(\boldsymbol{q})\boldsymbol{G}(\boldsymbol{q})\boldsymbol{\nu}, \tag{10.63}$$

and matrix

$$\boldsymbol{S}_t(\boldsymbol{q}) = \boldsymbol{J}_g(\boldsymbol{q})\boldsymbol{G}(\boldsymbol{q}) \tag{10.64}$$

is the sought $6 \times (6-k)$ selection matrix, being $\boldsymbol{J}_g(\boldsymbol{q})$ the 6×6 geometric Jacobian of the manipulator.

The geometric constraints (10.58) also allow introducing a set of $6-k$ independent coordinates $\boldsymbol{r}$ that, at least locally, describe the configuration of the robot in contact with the environment. In fact, from the implicit function theorem, a suitable $6-k$ vector function $\boldsymbol{r}(\boldsymbol{q})$ can be defined, such that the equations

$$\begin{aligned} \boldsymbol{0} &= \boldsymbol{h}(\boldsymbol{q}) \\ \boldsymbol{r} &= \boldsymbol{r}(\boldsymbol{q}) \end{aligned}$$

are independent at least locally in a neighborhood of the operating point. This allows defining the inverse mapping

$$\boldsymbol{q} = \boldsymbol{\rho}(\boldsymbol{r}), \tag{10.65}$$

and the differential mapping

$$\dot{\boldsymbol{q}} = \boldsymbol{Q}(\boldsymbol{r})\dot{\boldsymbol{r}}, \tag{10.66}$$

being $\boldsymbol{Q}$ the $6 \times (6-k)$ full-rank Jacobian $\boldsymbol{Q}(\boldsymbol{r}) = \partial\boldsymbol{\rho}/\partial\boldsymbol{r}$, with $\boldsymbol{A}\boldsymbol{Q} = \boldsymbol{O}$. Equation (10.66), at least locally, is equivalent to the mapping (10.62), with the choice $\boldsymbol{\nu} = \dot{\boldsymbol{r}}$ and $\boldsymbol{G}(\boldsymbol{q}) = \boldsymbol{Q}(\boldsymbol{r}(\boldsymbol{q}))$.

Hence, Eq. (10.63) can be rewritten in the equivalent form

$$\boldsymbol{t}_e = \boldsymbol{J}_g(\boldsymbol{\rho}(\boldsymbol{r}))\,\boldsymbol{Q}(\boldsymbol{r})\dot{\boldsymbol{r}} = \boldsymbol{S}_t(\boldsymbol{r})\dot{\boldsymbol{r}}, \tag{10.67}$$

being $\boldsymbol{S}_t(\boldsymbol{r}) = \boldsymbol{J}_g(\boldsymbol{\rho}(\boldsymbol{r}))\,\boldsymbol{Q}(\boldsymbol{r})$ the selection matrix computed as a function of the generalized coordinates $\boldsymbol{r}$. Similarly, $\boldsymbol{S}_w$ in (10.61) can be computed from $\boldsymbol{r}$ using (10.65).

The introduction of local generalized coordinates $\boldsymbol{r}$, on the one hand, facilitates the specification of an interaction task, in the case of rigid environment, assuming that the constraint equations (10.58) are known. On the other hand, it makes the task formulation strongly dependent on the contact model and the set of coordinates selected.

10.4 Hybrid Force/Motion Control

The reciprocity of the wrench and twist control subspaces naturally leads to a control approach, known as *hybrid force/motion control*, aimed at controlling simultaneously the contact force and the end-effector motion in two reciprocal subspaces.

10.4.1 Rigid Environment

In the presence of k geometric constraints, it is possible to reduce the description of the end-effector dynamics (10.60) to a submanifold of dimension $6-k$ using a mathematical derivation formally analogous to that of Sect. 5.10.

First, computing the time derivative of $\boldsymbol{t}_e = \boldsymbol{S}_t \boldsymbol{\nu}$ gives

$$\dot{\boldsymbol{t}}_e = \boldsymbol{S}_t(\boldsymbol{q})\dot{\boldsymbol{\nu}} + \dot{\boldsymbol{S}}_t(\boldsymbol{q})\boldsymbol{\nu},$$

which can be plugged into (10.60) to achieve

$$\boldsymbol{\Lambda}_g(\boldsymbol{q})\boldsymbol{S}_t(\boldsymbol{q})\dot{\boldsymbol{\nu}} + \boldsymbol{\kappa}_g(\boldsymbol{q},\dot{\boldsymbol{q}}) = \boldsymbol{w}_e - \boldsymbol{S}_w(\boldsymbol{q})\boldsymbol{\lambda}_{\text{env}}, \tag{10.68}$$

where

$$\boldsymbol{\kappa}_g(\boldsymbol{q},\dot{\boldsymbol{q}}) = \boldsymbol{\Gamma}_g(\boldsymbol{q},\dot{\boldsymbol{q}})\boldsymbol{t}_e + \boldsymbol{\eta}_g(\boldsymbol{q}) + \boldsymbol{\Lambda}_g(\boldsymbol{q})\dot{\boldsymbol{S}}_t(\boldsymbol{q})\boldsymbol{\nu}.$$

The equation of the reduced dynamics is obtained by multiplying from left Eq. (10.68) by $\boldsymbol{S}_t^T$, which gives

$$\left(\boldsymbol{S}_t^T(\boldsymbol{q})\boldsymbol{\Lambda}_g(\boldsymbol{q})\boldsymbol{S}_t(\boldsymbol{q})\right)\dot{\boldsymbol{\nu}} = \boldsymbol{S}_t^T(\boldsymbol{q})\left(\boldsymbol{w}_e - \boldsymbol{\kappa}_g(\boldsymbol{q},\dot{\boldsymbol{q}})\right), \tag{10.69}$$

being $\boldsymbol{S}_t^T\boldsymbol{S}_w = \boldsymbol{O}$. The $(6-k)\times(6-k)$ matrix $\boldsymbol{S}_t^T\boldsymbol{\Lambda}_g\boldsymbol{S}_t$, which is invertible and positive definite, represents the reduced task-space inertia of the constrained robot. Vector $\boldsymbol{\lambda}_{\text{env}}$ can be computed from (10.68) by multiplying from left that equation by matrix

$$(\boldsymbol{S}_w(\boldsymbol{q}))^{\dagger}_{\boldsymbol{\Lambda}_g} = (\boldsymbol{S}_w^T(\boldsymbol{q})\boldsymbol{\Lambda}_g^{-1}(\boldsymbol{q})\boldsymbol{S}_w(\boldsymbol{q}))^{-1}\boldsymbol{S}_w^T(\boldsymbol{q})\boldsymbol{\Lambda}_g^{-1}(\boldsymbol{q}),$$

which is the pseudoinverse of $\boldsymbol{S}_w$ weighted by matrix $\boldsymbol{\Lambda}_g$. This yields

$$\boldsymbol{\lambda}_{\text{env}} = (\boldsymbol{S}_w(\boldsymbol{q}))^{\dagger}_{\boldsymbol{\Lambda}_g}(\boldsymbol{w}_e - \boldsymbol{\kappa}_g(\boldsymbol{q},\dot{\boldsymbol{q}})). \tag{10.70}$$

Therefore, the control law

$$\boldsymbol{w}_e = \boldsymbol{\Lambda}_g(\boldsymbol{q})\boldsymbol{S}_t(\boldsymbol{q})\boldsymbol{\alpha}_{\boldsymbol{\nu}} + \boldsymbol{S}_w(\boldsymbol{q})\boldsymbol{w}_{\boldsymbol{\lambda}} + \boldsymbol{\kappa}_g(\boldsymbol{q},\dot{\boldsymbol{q}}), \tag{10.71}$$

with the external commands $\boldsymbol{\alpha}_{\boldsymbol{\nu}}$ and $\boldsymbol{w}_{\boldsymbol{\lambda}}$, cancels all nonlinearities and dynamics couplings and returns

$$\dot{\boldsymbol{\nu}} = \boldsymbol{\alpha}_{\boldsymbol{\nu}} \qquad \boldsymbol{\lambda}_{\text{env}} = \boldsymbol{w}_{\boldsymbol{\lambda}}, \tag{10.72}$$

showing a complete decoupling between twist and wrench control subspaces.

It should be noted that, in principle, for the implementation of control law (10.71), the constraint equation (10.58) is not required, provided that matrices $\boldsymbol{S}_w$ and $\boldsymbol{S}_t$ are known. These matrices could be computed on the basis of the geometry of the environment or can be estimated online, using force and velocity measurements.

The task can be assigned by specifying a desired wrench, through vector $\boldsymbol{\lambda}_d(t) = \boldsymbol{S}_w(\boldsymbol{q})\boldsymbol{w}_d(t)$, and a desired velocity, through vector $\boldsymbol{\nu}_d(t) = \boldsymbol{S}_t(\boldsymbol{q})\boldsymbol{t}_d(t)$.

The desired wrench can be achieved by setting

$$\boldsymbol{w}_{\boldsymbol{\lambda}} = \boldsymbol{\lambda}_d(t),$$

but this choice is very sensitive to disturbance forces, since it contains no force feedback. Alternative choices are

$$\boldsymbol{w}_{\boldsymbol{\lambda}} = \boldsymbol{\lambda}_d(t) - \boldsymbol{K}_{P\lambda}\big(\boldsymbol{\lambda}_d(t) - \boldsymbol{\lambda}_{\text{env}}(t)\big), \tag{10.73}$$

or

$$\boldsymbol{w}_{\boldsymbol{\lambda}} = \boldsymbol{\lambda}_d(t) + \boldsymbol{K}_{I\lambda}\int_0^t \big(\boldsymbol{\lambda}_d(\tau) - \boldsymbol{\lambda}_{\text{env}}(\tau)\big)d\tau, \tag{10.74}$$

where $\boldsymbol{K}_{P\lambda}$ and $\boldsymbol{K}_{I\lambda}$ are suitable positive definite, usually diagonal, gain matrices. The proportional feedback is able to reduce the force error due to disturbance forces. However, since the force loop in (10.72) is instantaneous, the gains of the diagonal matrix $\boldsymbol{K}_{P\lambda}$ must be set in the interval $(0, 1)$ to guarantee closed-loop stability in the presence of an arbitrarily small time delay, and this limits the benefits of force feedback. On the other hand, the integral action is able to compensate for constant bias disturbances and does not suffer from the limitations of proportional feedback (see Problem 10.10). The implementation of force feedback requires the computation of vector $\boldsymbol{\lambda}_{\text{env}}$ from the measurement of the end-effector wrench $\boldsymbol{w}_{\text{env}}$, using (10.54), i.e., $\boldsymbol{\lambda}_{\text{env}} = \boldsymbol{S}_w^{\dagger}\boldsymbol{w}_{\text{env}}$.

Motion control is achieved by setting

$$\boldsymbol{\alpha}_{\boldsymbol{\nu}} = \dot{\boldsymbol{\nu}}_d(t) + \boldsymbol{K}_{P\nu}\big(\boldsymbol{\nu}_d(t) - \boldsymbol{\nu}(t)\big) + \boldsymbol{K}_{I\nu}\int_0^t \big(\boldsymbol{\nu}_d(\tau) - \boldsymbol{\nu}(\tau)\big)d\tau, \tag{10.75}$$

where $\boldsymbol{K}_{P\nu}$ and $\boldsymbol{K}_{I\nu}$ are suitable gain matrices, usually diagonal. Hence, asymptotic tracking of $\boldsymbol{\nu}_d(t)$ and $\dot{\boldsymbol{\nu}}_d(t)$ is ensured with exponential convergence for any choice of positive definite matrices $\boldsymbol{K}_{P\nu}$ and $\boldsymbol{K}_{I\nu}$. Vector $\boldsymbol{\nu}$ is computed using (10.54), i.e., $\boldsymbol{\nu} = \boldsymbol{S}_t^{\dagger}\boldsymbol{t}_e$, where the end-effector twist $\boldsymbol{t}_e$ is computed from joint position and velocity measurements. The resulting scheme of *hybrid force/velocity control* is shown in Fig. 10.14, where $\boldsymbol{C}_w(s)$ and $\boldsymbol{C}_t(s)$ are the transfer matrices of the linear parts of the force and velocity controllers, respectively.

When the constraint equations (10.58) are available, matrices $\boldsymbol{S}_w$ and $\boldsymbol{S}_t$ can be computed using the analytic formulation. Moreover, a *hybrid force/position control* can be designed by specifying a desired $\boldsymbol{\lambda}_d(t)$, and a desired vector of coordinates $\boldsymbol{r}_d(t)$. The force control law can be designed as above, while a desired $\boldsymbol{r}_d$ can be

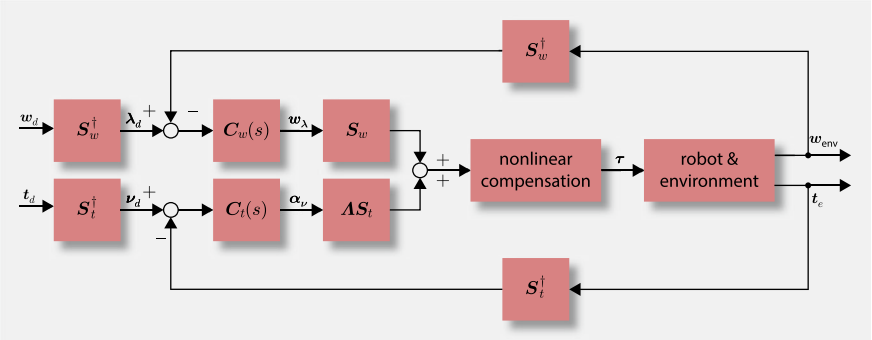

Fig. 10.14 Block diagram of hybrid force/velocity control for rigid environment

achieved with the choice

$$\boldsymbol{\alpha}_{\boldsymbol{\nu}} = \ddot{\boldsymbol{r}}_d + \boldsymbol{K}_{Dr}(\dot{\boldsymbol{r}}_d - \dot{\boldsymbol{r}}) + \boldsymbol{K}_{Pr}(\boldsymbol{r}_d - \boldsymbol{r}), \tag{10.76}$$

where $\boldsymbol{K}_{Dr}$ and $\boldsymbol{K}_{Pr}$ are suitable positive definite matrices and vector $\boldsymbol{r}$ can be computed from the joint position measurements using equation $\boldsymbol{r} = \boldsymbol{r}(\boldsymbol{q})$, while $\dot{\boldsymbol{r}} = \boldsymbol{\nu}$.

Finally, it is worth noting that the control torque $\boldsymbol{\tau} = \boldsymbol{J}_g^T(\boldsymbol{q})\boldsymbol{w}_e$, with $\boldsymbol{w}_e$ in (10.71), can be rewritten in a form similar to (10.33), but using geometric quantities, i.e.,

$$\boldsymbol{\tau} = \boldsymbol{J}_g^T(\boldsymbol{q})\boldsymbol{\gamma}_g + \boldsymbol{n}(\boldsymbol{q}, \dot{\boldsymbol{q}}), \tag{10.77}$$

where $\boldsymbol{\gamma}_g$ is the control wrench

$$\boldsymbol{\gamma}_g = \boldsymbol{\Lambda}_g(\boldsymbol{q})\left(\boldsymbol{S}_t(\boldsymbol{q})\boldsymbol{\alpha}_{\boldsymbol{\nu}} + \dot{\boldsymbol{S}}_t(\boldsymbol{q})\boldsymbol{\nu} - \dot{\boldsymbol{J}}(\boldsymbol{q})\dot{\boldsymbol{q}}\right) + \boldsymbol{S}_w(\boldsymbol{q})\boldsymbol{w}_{\boldsymbol{\lambda}}. \tag{10.78}$$

10.4.2 Compliant Environment

If the hypothesis of rigid contact is removed, along some task directions both motion and force are allowed, although they are not independent. Hybrid force/motion control schemes can be defined also in this case. For the sake of simplicity, the following assumptions are made.

- All the interaction forces are of elastic type, so that the wrench control subspace coincides with that of the elastic forces. This implies that the elastic contact wrench can be expressed as $\boldsymbol{w}_{\text{env}} = \boldsymbol{S}_w\boldsymbol{\lambda}_{\text{env}}$ as in the case of a rigid environment, although $\boldsymbol{\lambda}_{\text{env}}$ is no longer a vector of Lagrange multipliers.
- The local deformation of the environment is small and belongs to the orthogonal complement of the twist control subspace.
- The environment, in the undeformed configuration, is motionless, the selection matrices $\boldsymbol{S}_t$ and $\boldsymbol{S}_w$ are constant, and the compliance matrix is constant as well.

In view of the above assumptions, the end-effector elementary displacement, which coincides with the environment deformation is $\Delta \boldsymbol{t}_{re} = \boldsymbol{t}_e dt$, with $\boldsymbol{t}_e \in \mathcal{R}^{\perp}(\boldsymbol{S}_t)$ and can be computed as $\boldsymbol{t}_e dt = \boldsymbol{C}\boldsymbol{S}_w d\boldsymbol{\lambda}_{\text{env}} = \boldsymbol{C}\boldsymbol{S}_w \dot{\boldsymbol{\lambda}}_{\text{env}} dt$, being $\boldsymbol{C}$ is the constant positive semi-definite compliance matrix of the environment, with $\boldsymbol{S}_t^T \boldsymbol{C} = \boldsymbol{O}$. Therefore, the end-effector twist can be decomposed into the sum of two orthogonal vectors

$$\boldsymbol{t}_e = \boldsymbol{S}_t \boldsymbol{\nu} + \boldsymbol{C}\boldsymbol{S}_w \dot{\boldsymbol{\lambda}}_{\text{env}}. \tag{10.79}$$

The elastic energy stored at the contact is

$$\mathcal{U}_e = \frac{1}{2} \boldsymbol{w}_{\text{env}}^T \boldsymbol{C} \boldsymbol{w}_{\text{env}} = \frac{1}{2} \boldsymbol{\lambda}_{\text{env}}^T \boldsymbol{S}_w^T \boldsymbol{C} \boldsymbol{S}_w \boldsymbol{\lambda}_{\text{env}} > 0 \quad \text{for all } \boldsymbol{\lambda}_{\text{env}} \neq \boldsymbol{0},$$

where the $k \times k$ matrix $\boldsymbol{S}_w^T \boldsymbol{C} \boldsymbol{S}_w$ is positive definite.

The task space control law based on feedback linearization

$$\boldsymbol{w}_e = \boldsymbol{\Lambda}_g(\boldsymbol{q}) \boldsymbol{a}_e + \boldsymbol{\Gamma}_g(\boldsymbol{q}, \dot{\boldsymbol{q}}) \boldsymbol{t}_e + \boldsymbol{\eta}_g(\boldsymbol{q}) + \boldsymbol{S}_w(\boldsymbol{q}) \boldsymbol{\lambda}_{\text{env}}, \tag{10.80}$$

with the external command $\boldsymbol{a}_e$, leads to the linear equation

$$\dot{\boldsymbol{t}}_e = \boldsymbol{a}_e. \tag{10.81}$$

The corresponding control torque $\boldsymbol{\tau} = \boldsymbol{J}_g^T(\boldsymbol{q}) \boldsymbol{w}_e$ can be expressed in the form (10.77), with

$$\gamma_g = \boldsymbol{\Lambda}_g(\boldsymbol{q})(\boldsymbol{a}_e - \dot{\boldsymbol{J}}(\boldsymbol{q}) \dot{\boldsymbol{q}}) + \boldsymbol{S}_w(\boldsymbol{q}) \boldsymbol{w}_{\boldsymbol{\lambda}}. \tag{10.82}$$

Computing the time derivative of $\boldsymbol{t}_e$ in (10.79) and using (10.81) gives

$$\boldsymbol{S}_t \dot{\boldsymbol{\nu}} + \boldsymbol{C}\boldsymbol{S}_w \ddot{\boldsymbol{\lambda}}_{\text{env}} = \boldsymbol{a}_e. \tag{10.83}$$

Choosing the control input $\boldsymbol{\alpha}$ with the same structure of the left hand side of (10.83), with external commands $\boldsymbol{\alpha}_{\boldsymbol{\nu}}$ and $\boldsymbol{w}_{\boldsymbol{\lambda}}$, i.e.,

$$\boldsymbol{a}_e = \boldsymbol{S}_t \boldsymbol{\alpha}_{\boldsymbol{\nu}} + \boldsymbol{C}\boldsymbol{S}_w \boldsymbol{w}_{\boldsymbol{\lambda}}, \tag{10.84}$$

yields the two decoupled equations

$$\dot{\boldsymbol{\nu}} = \boldsymbol{\alpha}_{\boldsymbol{\nu}} \qquad \ddot{\boldsymbol{\lambda}}_{\text{env}} = \boldsymbol{w}_{\boldsymbol{\lambda}}. \tag{10.85}$$

The equation of the left, representing the dynamics in the twist control subspace of dimension $6 - k$, is obtained from (10.83) and (10.84) after left-multiplication by $\boldsymbol{S}_t^T$, being $\boldsymbol{S}_t^T \boldsymbol{S}_t$ nonsingular. The equation on the right, representing the dynamics in the wrench control subspace of dimension k, is obtained after left multiplication by $\boldsymbol{S}_w^T$, being $\boldsymbol{S}_w^T \boldsymbol{C} \boldsymbol{S}_w$ nonsingular.

Note that, if only an estimate $\widehat{\boldsymbol{C}}$ of the compliance of the environment is available, but contact geometry is known, so that $\boldsymbol{S}_t^T \widehat{\boldsymbol{C}} = \boldsymbol{O}$, control law (10.84) can be rewritten in the form

$$\boldsymbol{a}_e = \boldsymbol{S}_t \boldsymbol{\alpha}_{\boldsymbol{\nu}} + \widehat{\boldsymbol{C}} \boldsymbol{S}_w \boldsymbol{w}_{\boldsymbol{\lambda}}. \tag{10.86}$$

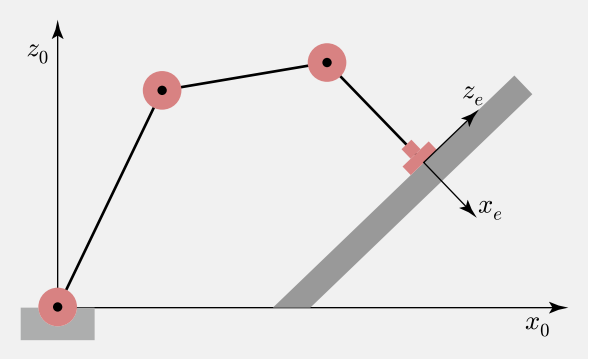

Fig. 10.15 3R planar arm in contact with an elastically compliant plane

In this case, the closed-loop equations (10.85) are replaced by the equations

$$\dot{\boldsymbol{\nu}} = \boldsymbol{\alpha}_{\boldsymbol{\nu}} \qquad \ddot{\boldsymbol{\lambda}}_{\text{env}} = (\boldsymbol{S}_w^T \boldsymbol{C} \boldsymbol{S}_w)^{-1} \boldsymbol{S}_w^T \widehat{\boldsymbol{C}} \boldsymbol{S}_w \boldsymbol{w}_{\boldsymbol{\lambda}}, \tag{10.87}$$

showing that the force and velocity control subspaces remain decoupled.

Example 10.4 Consider a 3R planar arm in contact with a purely frictionless elastic plane through a T-shaped end-effector (Fig. 10.15). The end-effector frame e is set as in the figure and coincides with frame r attached to the plane in the undeformed configuration. The task frame is set attached to the end-effector frame.

It assumed that the plane is compliant along axis x_t and about axis z_t of the task frame, and that the elastic behavior is decoupled. It is straightforward to recognize that the selection matrices $\boldsymbol{S}_t$ and $\boldsymbol{S}_w$, as well as the compliance matrix $\boldsymbol{C}$, are constant when expressed in the end-effector frame, which coincides with the task frame. Thus, in the design of the control law, it is convenient to refer all quantities to the end-effector frame. In detail, Eq. (10.79) can be rewritten as

$$^e\boldsymbol{t}_e = \boldsymbol{S}_t \boldsymbol{\nu} + \boldsymbol{C} \boldsymbol{S}_w \dot{\boldsymbol{\lambda}}_{\text{env}}$$

with constant $\boldsymbol{S}_t$, $\boldsymbol{S}_w$ and $\boldsymbol{C}$, whose time derivative is

$$^e\dot{\boldsymbol{t}}_e = \boldsymbol{S}_t \dot{\boldsymbol{\nu}} + \boldsymbol{C} \boldsymbol{S}_w \ddot{\boldsymbol{\lambda}}_{\text{env}}.$$

On the other hand, equation $\dot{\boldsymbol{t}}_e = \boldsymbol{a}_e$ can be rewritten in the form

$$\bar{\boldsymbol{R}}_e \, ^e\dot{\boldsymbol{t}}_e + \dot{\bar{\boldsymbol{R}}}_e \, ^e\boldsymbol{t}_e = \boldsymbol{a}_e.$$

Then, choosing

$$\boldsymbol{a}_e = \bar{\boldsymbol{R}}_e \, ^e\boldsymbol{\alpha}_e + \dot{\bar{\boldsymbol{R}}}_e \, ^e\boldsymbol{t}_e,$$

where $^e\boldsymbol{\alpha}_e$ is a new control input, yields

$$\boldsymbol{S}_t \dot{\boldsymbol{\nu}} + \boldsymbol{C} \boldsymbol{S}_w \ddot{\boldsymbol{\lambda}}_{\text{env}} = {}^e\boldsymbol{\alpha}_e,$$

which is the counterpart of (10.83) in the end-effector frame. At this point, the control input ${}^e\boldsymbol{\alpha}_e$ can be set as in (10.84) referring all quantities to the end-effector frame, and this leads to the same decoupled equations for $\dot{\boldsymbol{\nu}}$ and $\ddot{\boldsymbol{\lambda}}_{\text{env}}$.

Concerning matrices $\boldsymbol{S}_t$, $\boldsymbol{S}_w$, $\boldsymbol{C}$, in view of the planar arm's kinematics, it is relevant to consider only the components of linear velocity along axes x_e and y_e and the component of angular velocity about axis z_e. Therefore, matrices $\boldsymbol{S}_t$ and $\boldsymbol{S}_w$ can be defined as

$$\boldsymbol{S}_t = \boldsymbol{e}_2 \qquad \boldsymbol{S}_w = \begin{pmatrix} \boldsymbol{e}_1 & \boldsymbol{e}_3 \end{pmatrix}$$

being $\boldsymbol{e}_i \in I\!R^3$ the unit vector with 1 in the i-th entry and 0 in all the others. The compliance matrix $\boldsymbol{C}$ can be built by considering a linear spring along axis x_e and a torsional spring about axis z_e acting in parallel, i.e.,

$$\boldsymbol{C} = c_t \boldsymbol{e}_1 \boldsymbol{e}_1^T + c_o \boldsymbol{e}_3 \boldsymbol{e}_3^T = \begin{pmatrix} c_t & 0 & 0 \\ 0 & 0 & 0 \\ 0 & 0 & c_o \end{pmatrix},$$

being c_t the translational compliance and c_o the rotational compliance. Note that $\boldsymbol{S}_t^T \boldsymbol{C} = \boldsymbol{O}$, and

$$\boldsymbol{S}_w^T \boldsymbol{C} \boldsymbol{S}_w = \begin{pmatrix} c_t & 0 \\ 0 & c_o \end{pmatrix}$$

is a positive definite matrix.

If the compliance coefficients are uncertain, using $\hat{c}_t$ and $\hat{c}_o$ in the control input, the closed-loop equation in the force control subspace must be replaced by

$$\ddot{\boldsymbol{\lambda}}_{\text{env}} = \begin{pmatrix} c_t & 0 \\ 0 & c_o \end{pmatrix}^{-1} \begin{pmatrix} \hat{c}_t & 0 \\ 0 & \hat{c}_o \end{pmatrix} \boldsymbol{w}_{\boldsymbol{\lambda}} = \begin{pmatrix} \hat{c}_t/c_t & 0 \\ 0 & \hat{c}_o/c_o \end{pmatrix} \boldsymbol{w}_{\boldsymbol{\lambda}}.$$

■

As for the rigid environment case, the task can be assigned by specifying a desired wrench, in terms of vector $\boldsymbol{\lambda}_d(t) = \boldsymbol{S}_w^{\dagger} \boldsymbol{w}_d(t)$, and a desired twist, in terms of vector $\boldsymbol{\nu}_d(t) = \boldsymbol{S}_w^{\dagger} \boldsymbol{w}_d(t)$. The overall hybrid force/velocity control scheme can be represented as in Fig. 10.16. Note that the control action in the wrench control subspace is transformed into a twist by the available estimate $\widehat{\boldsymbol{C}}$ of the compliance matrix to be added to the control action in the twist control subspace. Vice versa, in the rigid environment scheme shown in Fig. 10.14, the control action in the twist control subspace is transformed into a wrench by the inertia matrix $\boldsymbol{\Lambda}_g$ to be added to the control action in the wrench control subspace.

The control input $\boldsymbol{\alpha}_{\boldsymbol{\nu}}$ can be selected as in the rigid contact case by using (10.75), while the design of $\boldsymbol{w}_{\boldsymbol{\lambda}}$ should be made taking into account that force and velocity are related to the compliance of the environment.

In detail, considering for simplicity the control of a single force component, and assuming complete decoupling of compliant behavior, the time derivative of the force λ_{env} is related to the end-effector velocity along the same direction ν by the stiffness $k = c^{-1}$, i.e., $\dot{\lambda}_{\text{env}} = k\nu$. This allows avoiding the force derivative feedback, which

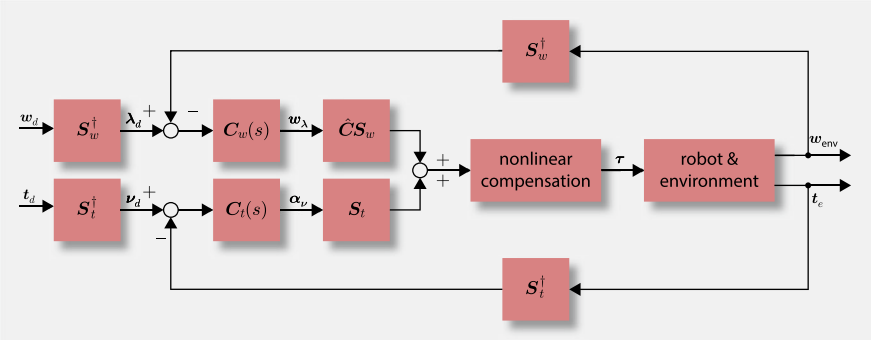

Fig. 10.16 Block diagram of hybrid force/velocity control for compliant environment

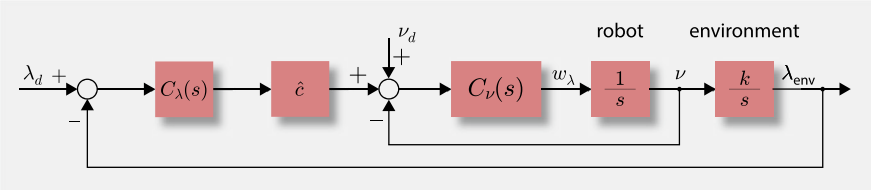

Fig. 10.17 Block diagram in the Laplace domain of the linear force control ($\nu_d = 0$) for a single interaction direction in the presence of elastic environment. When a desired velocity is provided as input ($\nu_d \neq 0$), the scheme is a parallel force/motion control

can be replaced by a velocity feedback, as long as an estimate $\hat{c}$ of the compliance of the environment is available. Hence, the overall linear control scheme for the single component consists of an inner velocity controller with transfer function $C_\nu(s)$ and an outer force controller with transfer function $C_\lambda(s)$, to be designed in a suitable way. The resulting block diagram, reported in Fig. 10.17, resembles the admittance control scheme of Fig. 10.6, where the robot admittance is an integrator $Y_r(s) = 1/s$, the environment impedance is $Z_e(s) = k/s$ and a desired force λ_d is specified in place of a desired velocity ν_d. In the case $\nu_d \neq 0$ the scheme is known as *parallel force/motion control*.

The admittance of the controlled robot from force $-\lambda_{\text{env}}$ to velocity ν can be easily computed from the block diagram in Fig. 10.17, and has the expression

$$Y_c(s) = \frac{C_\nu(s)C_\lambda(s)\hat{c}}{s + C_\nu(s)}, \tag{10.88}$$

while the closed-loop transfer function from λ_d to λ is

$$W(s) = \frac{C_\nu(s)C_\lambda(s)\hat{c}k}{s^2 + C_\nu(s)s + C_\nu(s)C_\lambda(s)\hat{c}k}. \tag{10.89}$$

Different choices are possible for the linear controllers $C_\nu(s)$ and $C_\lambda(s)$. For instance:

- proportional control on both velocity and force

$$C_\nu(s) = k_P \qquad C_\lambda(s) = k_F; \tag{10.90}$$

- PI control on velocity and proportional control on force

$$C_\nu(s) = k_P + \frac{k_I}{s} \qquad C_\lambda(s) = k_F; \tag{10.91}$$

- PI control on both velocity and force

$$C_\nu(s) = k_P + \frac{k_I}{s} \qquad C_\lambda(s) = k_{PF} + \frac{k_{IF}}{s}. \tag{10.92}$$

All options ensure that the contact force is equal to a desired constant force λ_d in steady state, i.e., $W(0) = 1$ even in case $\hat{c}k \neq 1$. Furthermore, if a good estimate of the stiffness of the environment is available, i.e., $\hat{c} = k^{-1}$, transfer function (10.89) is independent of k, as are the stability and transient performance.

With control laws (10.90), the closed-loop transfer function (10.89) becomes

$$W(s) = \frac{k_P k_F \hat{c}k}{s^2 + k_P s + k_P k_F \hat{c}k},$$

which is that of a typical second-order system. Hence, assuming $\hat{c}k = 1$, with a suitable choice of the two gains k_P and k_F, it is possible to arbitrarily set the natural frequency ω_n and the damping ratio ζ (see Appendix D.1). Asymptotic stability is also guaranteed in the case $\hat{c}k \neq 1$, if and only if $k_P > 0$ and $k_F > 0$. It should be noted that, under the same conditions, the admittance of the controlled robot (10.88) is SPR (see Problem 10.11); therefore, asymptotic stability is ensured in case of interaction with any passive environment, even if not purely elastic.

With control laws (10.91), the integral action on the inner velocity control loop guarantees a better rejection of joint friction and other unmodeled disturbances. The transfer function (10.89) is

$$W(s) = \frac{k_F(k_I + k_P s)\hat{c}k}{s^3 + k_P s^2 + (k_I + k_P k_F \hat{c}k)s + k_I k_F \hat{c}k}.$$

The choice of the control gains is more elaborated than in the previous case, but can be carried out using standard design tools for linear control systems. From the Routh–Hurwitz criterion (see Appendix D.1), it follows that asymptotic stability is ensured if and only if the gains $k_P > 0$, $k_I > 0$ and $k_F > 0$ are set so that $k_P k_I > (k_I - k_P^2)k_F \hat{c}\, k$. Hence, choosing $k_I < k_P^2$, asymptotic stability is guaranteed for any value of the stiffness k. If the latter inequality is satisfied, the admittance of the controlled robot (10.88) is SPR (see Problem 10.12) and asymptotic stability is

also ensured in case of interaction with any passive environment, even if not purely elastic.

With control laws (10.92), the presence of the integral action in the outer force control loop guarantees a steady-state null force error, also in the presence of constant bias disturbances. The control design can be simplified by using a modified force controller with transfer function:

$$C'_{\lambda}(s) = \frac{s^2 + k_P s + k_I}{(k_P s + k_I)(1 + \tau_F s)} C_{\lambda}(s), \tag{10.93}$$

where $C_{\lambda}(s)$ is set as in (10.92) and the pole $s = -1/\tau_F$, with $\tau_F > 0$, ensures that $C'_{\lambda}(s)$ is a proper transfer function. Using this controller, the transfer function (10.89) becomes

$$W(s) = \frac{(k_{IF} + k_{PF} s)\hat{c}k}{\tau_F s^3 + s^2 + k_{PF}\hat{c}k s + k_{IF}\hat{c}k},$$

which does not depend on the gains of the velocity control loop. The latter can be designed independently on the force control loop, making it easier to guarantee asymptotic stability and satisfactory performance. From the Routh–Hurwitz criterion it follows that asymptotic stability is ensured if and only if the gains $k_{PF} > 0$, $k_{IF} > 0$ and $\tau_F > 0$ satisfy the inequality $k_{PF} > k_{IF}\tau_F$, independently of the stiffness k. It can be shown that, if these gain conditions are satisfied, the admittance of the controlled robot is at most PR (see Problem 10.13). Hence, in the case of interaction with a passive environment that is not purely elastic, only marginal stability is guaranteed.

Finally, it should be noted that the inner velocity control law is the same as that adopted in the twist control subspace (10.75), except for the acceleration feedforward. This allows using the same inner control law for the velocity components along all the directions of the task frame. As for the outer force control loop, although it can be left active in all the task directions, it operates only in the directions of interaction. This approach is known as *parallel force/position control*, and is represented by the block diagram in Fig. 10.17 with $\nu_d \neq 0$.

10.5 The Case of Redundant Robots

Force control strategies are typically designed in task space. If the robot is redundant with respect to the interaction task, then it is possible to pursue other auxiliary goals or satisfy additional constraints, possibly with priorities (see Chap. 3 and Sect. 6.5.3). Usually, the interaction task is the one with the highest priority, although this is not always the case; also, physical interaction with simultaneous contacts on different parts of the robot could happen.

The task-space control approaches of this chapter focus on a single interaction task, assuming that the robot is nonredundant, but it can be easily extended to the case of redundant robots.

That is, task-space compliance control, with and without force feedback, based on (10.24), with (10.25) or (10.27), can be employed also for redundant robots (see Problem 10.7). The stability of null-space motion is guaranteed in the presence of dissipative torques caused by joint friction; damping contributions can be added to the control torques if necessary. Redundancy can be exploited by introducing an additional contribution to the control torque, i.e., using

$$\boldsymbol{\tau} = \boldsymbol{J}^T(\boldsymbol{q})\boldsymbol{\gamma} + (\boldsymbol{I} - \boldsymbol{J}_{\boldsymbol{M}}^{\dagger}\boldsymbol{J})^T\boldsymbol{\tau}_N + \boldsymbol{g}(\boldsymbol{q}), \tag{10.94}$$

where $\boldsymbol{\gamma}$ is chosen according to (10.25) or (10.27), $\boldsymbol{\tau}_N$ is a suitable null-space torque and $\boldsymbol{J}_{\boldsymbol{M}}^{\dagger}$ is the *dynamically consistent* pseudoinverse of $\boldsymbol{J}$, defined as

$$\boldsymbol{J}_{\boldsymbol{M}}^{\dagger} = \boldsymbol{M}^{-1}\boldsymbol{J}^T(\boldsymbol{J}\boldsymbol{M}^{-1}\boldsymbol{J}^T)^{-1} = \boldsymbol{M}^{-1}\boldsymbol{J}^T\boldsymbol{\Lambda}.$$

The dynamic consistency property (5.138), with (5.139), ensures that the task-space dynamics of the controlled robot, in the presence of the interaction force $\boldsymbol{\gamma}_{\text{env}}$, is still described by the nonlinear impedance (10.29). However, closed-loop stability of the overall system is not easy to prove analytically and depends also on the choice of the null-space torque $\boldsymbol{\tau}_N$.

Similar considerations can be made for impedance control based on (10.24) and (10.30), with task space impedance (10.31).

For impedance control with force feedback and admittance control, based on feedback linearization in task space (10.33) and (10.34), redundancy can be exploited by replacing (10.33) with control torque

$$\boldsymbol{\tau} = \boldsymbol{J}^T(\boldsymbol{q})\boldsymbol{\gamma} + (\boldsymbol{I} - \boldsymbol{J}_{\boldsymbol{M}}^{\dagger}\boldsymbol{J})^T\boldsymbol{\tau}_N + \boldsymbol{n}(\boldsymbol{q}, \dot{\boldsymbol{q}}), \tag{10.95}$$

which has the same structure of the linearizing torque (6.106).

It is possible to derive a task priority control solution analogous to the prioritized solution (3.80) for two tasks, which can be easily extended to multiple tasks. In detail, two tasks are described at the first-order differential level by

$$\dot{\boldsymbol{y}}_1 = \boldsymbol{J}_1(\boldsymbol{q})\dot{\boldsymbol{q}} \qquad \dot{\boldsymbol{y}}_2 = \boldsymbol{J}_2(\boldsymbol{q})\dot{\boldsymbol{q}},$$

with task velocities $\dot{\boldsymbol{y}}_1 \in I\!R^{m_1}$ and $\dot{\boldsymbol{y}}_2 \in I\!R^{m_2}$, and full rank $\boldsymbol{J}_1$ and $\boldsymbol{J}_2$. Let task 1 be of higher priority than task 2; also, assume that the interaction force $\boldsymbol{\gamma}_{\text{env}}$ performs work only on task variables $\boldsymbol{y}_1$ and that $\boldsymbol{J}_1$ is the corresponding contact Jacobian.

To simplify notation, use

$$\boldsymbol{P}_{1\boldsymbol{M}} = \boldsymbol{I} - \boldsymbol{J}_{1\boldsymbol{M}}^{\dagger}\boldsymbol{J}_1$$

to denote the projection matrix in the null space of $\boldsymbol{J}_1$ computed with the dynamically consistent pseudoinverse of $\boldsymbol{J}_1$. In view of (6.111), it is

$$\boldsymbol{M}\boldsymbol{P}_{1\boldsymbol{M}}\boldsymbol{M}^{-1} = \boldsymbol{P}_{1\boldsymbol{M}}^T \qquad \boldsymbol{M}^{-1}\boldsymbol{P}_{1\boldsymbol{M}}^T = \boldsymbol{P}_{1\boldsymbol{M}}\boldsymbol{M}^{-1}.$$

Considering (10.34) and (10.95), the control torque can be chosen as

$$\boldsymbol{\tau} = \boldsymbol{\tau}_1 + \boldsymbol{J}_1^T(\boldsymbol{q})\boldsymbol{\gamma}_{\text{env}} + \boldsymbol{P}_{1\boldsymbol{M}}^T(\boldsymbol{q})\boldsymbol{\tau}_N + \boldsymbol{n}(\boldsymbol{q}, \dot{\boldsymbol{q}}), \tag{10.96}$$

where $\boldsymbol{\tau}_1$ is the torque required to address task 1

$$\boldsymbol{\tau}_1 = \boldsymbol{J}_1^T(\boldsymbol{q})\boldsymbol{\Lambda}_1(\boldsymbol{q})\big(\boldsymbol{a}_{1\boldsymbol{y}} - \dot{\boldsymbol{J}}_1(\boldsymbol{q})\dot{\boldsymbol{q}}\big). \tag{10.97}$$

In the above equation, $\boldsymbol{\Lambda}_1 = (\boldsymbol{J}_1\boldsymbol{M}^{-1}\boldsymbol{J}_1^T)^{-1}$ is the inertia of the robot projected on the task 1 and $\boldsymbol{a}_{1\boldsymbol{y}}$ is a control input with the meaning of acceleration of task 1.

Plugging (10.96) into the dynamic model (10.18) with $\boldsymbol{B}_v = \boldsymbol{O}$ and $\boldsymbol{\tau}_{\text{env}} = \boldsymbol{J}_1^T\boldsymbol{\gamma}_{\text{env}}$, and computing the joint acceleration gives

$$\ddot{\boldsymbol{q}} = \boldsymbol{M}^{-1}\boldsymbol{\tau}_1 + \boldsymbol{M}^{-1}\boldsymbol{P}_{1\boldsymbol{M}}^T\boldsymbol{\tau}_N = \boldsymbol{M}^{-1}\boldsymbol{\tau}_1 + \boldsymbol{P}_{1\boldsymbol{M}}\boldsymbol{M}^{-1}\boldsymbol{\tau}_N. \tag{10.98}$$

Hence, computing the task 1 acceleration as

$$\ddot{\boldsymbol{y}}_1 = \dot{\boldsymbol{J}}_1\ddot{\boldsymbol{q}} + \boldsymbol{J}_1\dot{\boldsymbol{q}}$$

and using (10.97) and (10.98), one obtains $\ddot{\boldsymbol{y}}_1 = \boldsymbol{a}_{1\boldsymbol{y}}$, being $\boldsymbol{J}_1\boldsymbol{P}_{1\boldsymbol{M}} = \boldsymbol{O}$. Next, substituting the solution $\ddot{\boldsymbol{q}}$ from (10.98) into the second desired task $\ddot{\boldsymbol{y}}_2 = \boldsymbol{a}_{2\boldsymbol{y}}$ gives the equation

$$\boldsymbol{a}_{2\boldsymbol{y}} = \ddot{\boldsymbol{y}}_2 = \boldsymbol{J}_2\ddot{\boldsymbol{q}} + \dot{\boldsymbol{J}}_2\dot{\boldsymbol{q}} = \boldsymbol{J}_2\boldsymbol{M}^{-1}\boldsymbol{\tau}_1 + \boldsymbol{J}_2\boldsymbol{P}_{1\boldsymbol{M}}\boldsymbol{M}^{-1}\boldsymbol{\tau}_N + \dot{\boldsymbol{J}}_2\dot{\boldsymbol{q}}$$

which, choosing $\boldsymbol{\tau}_N = \boldsymbol{P}_{1\boldsymbol{M}}^T\boldsymbol{J}_2^T\boldsymbol{\gamma}_2$, can be rearranged as

$$\boldsymbol{\Lambda}_{21}^{-1}\boldsymbol{\gamma}_2 = \boldsymbol{a}_{2\boldsymbol{y}} - \dot{\boldsymbol{J}}_2\dot{\boldsymbol{q}} - \boldsymbol{J}_2\boldsymbol{M}^{-1}\boldsymbol{\tau}_1,$$

being

$$\boldsymbol{\Lambda}_{21}(\boldsymbol{q}) = \Big(\boldsymbol{J}_2(\boldsymbol{q})\boldsymbol{P}_{1\boldsymbol{M}}(\boldsymbol{q})\boldsymbol{M}^{-1}(\boldsymbol{q})\boldsymbol{P}_{1\boldsymbol{M}}^T(\boldsymbol{q})\boldsymbol{J}_2^T(\boldsymbol{q})\Big)^{-1}$$

a projected inertia matrix. Therefore, torque $\boldsymbol{\tau}_2 = \boldsymbol{J}_2^T\boldsymbol{\gamma}_2$ can be computed as

$$\boldsymbol{\tau}_2 = \boldsymbol{J}_2^T(\boldsymbol{q})\boldsymbol{\Lambda}_{21}(\boldsymbol{q})\big(\boldsymbol{a}_{2\boldsymbol{y}} - \dot{\boldsymbol{J}}_2(\boldsymbol{q})\dot{\boldsymbol{q}} - \boldsymbol{J}_2(\boldsymbol{q})\boldsymbol{M}^{-1}(\boldsymbol{q})\boldsymbol{\tau}_1\big). \tag{10.99}$$

To conclude, considering that projection matrices are idempotent, control torque (10.96) can be rewritten replacing $\boldsymbol{\tau}_N$ with $\boldsymbol{\tau}_2$, namely

$$\boldsymbol{\tau} = \boldsymbol{\tau}_1 + \boldsymbol{J}_1^T(\boldsymbol{q})\boldsymbol{\gamma}_{\text{env}} + \boldsymbol{P}_{1\boldsymbol{M}}^T(\boldsymbol{q})\boldsymbol{\tau}_2 + \boldsymbol{n}(\boldsymbol{q}, \dot{\boldsymbol{q}}), \tag{10.100}$$

with $\boldsymbol{\tau}_1$ in (10.97), $\boldsymbol{\tau}_2$ in (10.99), and task 1 has higher priority than task 2. In case of multiple tasks, a hierarchical recursive formulation can be easily derived.

Finally, it should be noted that the same strategy can also be implemented for the hybrid force/motion schemes of Sect. 10.4, starting from the control torque (10.77).

Further Reading

Scientific publications on force control are numerous and cover a time period of about five decades. A description of the state of the art of the first decade is provided in [282], while the progress of the second and third decades is surveyed in [82]. More recent overviews can be found in [43,271], the latter including robots with elastic joints and series elastic actuators. Monographs on this subject are [109,242].

The control based on the concept of compliance was originally proposed by [188] in the joint space and [220] in the Cartesian space. The original idea of a mechanical impedance model used to control the interaction between the manipulator and the environment is presented in [114] while a compliant motion formulation can be found in [129]. The stability of impedance and admittance control based on passivity for rigid and elastic joint robots is discussed in [58,115,130,189,202].

The RCC concept is presented in [67] and its use for assembling operation is discussed in [281]. A reference paper for modeling 6-DoF elastic systems is [162] and their properties are analyzed in [96,206,256]. Models of elastic systems with semi-definite stiffness and compliance matrices are presented in [205]. For spatial rotations and translations, the specification of task-relevant impedance (and especially stiffness) is particularly challenging. This problem is addressed, e.g., in [39], as well as in the monograph [186]. Compliance control of redundant robots in a multi-priority framework is considered in [203,219].

Early works on force control using force feedback are described in [280] and instability problems related to force feedback are evidenced in [91]. The original idea of the hybrid force and position control is introduced in [214], based on the concepts of natural and artificial constraints proposed in [175]. The concept of reciprocity of forces and velocity is discussed in [159], while invariance problems are analyzed in [87]. The task frame formalism is developed in [33,85], as well as in [84] in the presence of geometric uncertainty. The explicit inclusion of the dynamic model of the manipulator, also for redundant robots, is presented in the seminal work [139]. The inclusion of constraints in the manipulator dynamics is considered in [177,285,287]. The use of impedance control in a hybrid framework is discussed in [7]. A systematic approach to modeling the interaction with a dynamic environment is developed in [75]. Adaptive versions of force/motion control schemes are proposed in [270].

The case of complex contact situations and time-varying constraints is presented in [34]. In [83,260] the issue of controlling contact transitions is discussed. Approaches that do not require exact knowledge of the environment model are force control with position feedforward [86] and parallel force/position control [51,54].

Problems

10.1 Analyze the passivity of impedance (10.12).

10.2 The simplified model of a robot with elastic transmission is represented in Fig. 10.18, where m_m is the mass of the motor and m is the mass of the link. Control

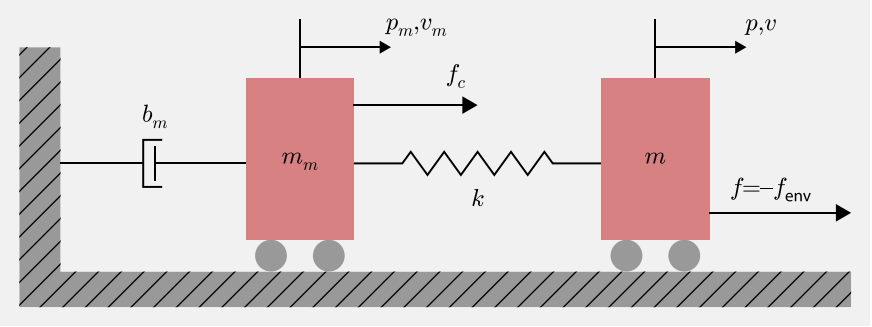

Fig. 10.18 Simplified model of a robot with elastic transmission

force f_c acts on the motor while the force f applied by the environment on the robot acts on the link. The parameter k is the stiffness coefficient of the transmission. Prove that the PD control law

$$f_c = k_d(p_d - p_m) + b_d(v_d - v_m),$$

based on feedback of the motor position p_m and velocity v_m, defines a passive impedance (or admittance) between the link (and environment) velocity $v = \dot{p}$ and the interaction force $f = -f_{\text{env}}$. To simplify the analysis, assume $b_m = 0$.

10.3 For a robot with elastic transmission, assuming $b_m = 0$, show that control law (10.13) with feedback of force f_{env} and of the motor variables p_m and v_m, with control gains $k_d > 0$ and $b_d > 0$, defines a passive impedance (or admittance) between the link (and environment) velocity $v = \dot{p}$ and the interaction force $f = -f_{\text{env}}$, provided that $k_F \in [0, 1]$.

10.4 Compute the admittance $Y(s)$ in (10.15) from the block diagram of Fig. 10.6.

10.5 Consider a PI velocity controller with transfer function

$$C_v(s) = k_p + \frac{k_i}{s},$$

and assume that the second term of (10.15) is null, i.e., the contact force is canceled by the controller. Set $k_p = \alpha_v m$ and $k_i = \alpha_v b$, with $\alpha_v > 0$ so that the zero in $s = -b/m$ of the velocity controller cancels out the pole of $Y_r(s)$ and (10.15) becomes

$$Y(s) = \frac{\alpha_v}{\alpha_v + s} C_f.$$

Show that, by setting $C_f(s) = Y_d(s)$ in (10.17), the passivity of the apparent admittance $Y(s)$ is not always guaranteed. In particular, prove that the PR condition fails in case of pure inertia, i.e., if $Y_d(s) = 1/m_d s$ and for any other desired

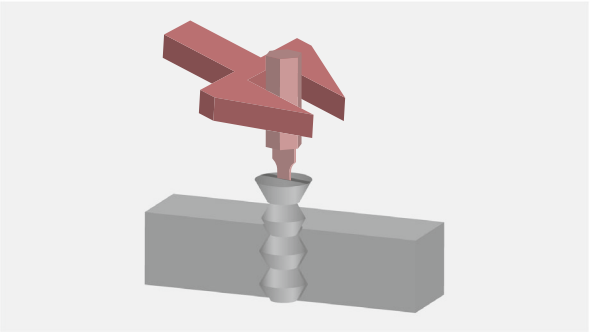

Fig. 10.19 Driving a screw in a hole

admittance containing an inertial contribution. Moreover, prove that the apparent admittance is SP if $k_d = 0$ and $b_d > 0$ and PR if $k_d \geq 0$ and $b_d \geq 0$.

10.6 Prove that a PR or SPR apparent admittance in the case $m_d > 0$ can be achieved by considering the same controller $C_v(s)$ of Problem 10.5 and setting

$$C_f(s) = \frac{s + \alpha_v}{\alpha_v} Y_d(s).$$

10.7 For the task considered in Example 10.2, analyze passivity and stability of compliance control assuming that the robot is redundant, e.g., is a 3R planar arm. [*Hint*: Show that compliance control (10.24), (10.25) ensures passivity of the controlled robot from input $\dot{\boldsymbol{q}}$ to output $-\boldsymbol{\tau}_{\text{env}} = -\boldsymbol{J}^T(\boldsymbol{q})\boldsymbol{\gamma}_{\text{env}}$.]

10.8 Show that the equilibrium equations for a robot with compliance or impedance control in contact with a 6-DoF elastic environment are (10.52) and (10.53).

10.9 For the manipulation task of driving a screw in a hole illustrated in Fig. 10.19, find the natural constraints and artificial constraints with respect to a suitably chosen task frame.

10.10 Considering the case of a single force component, show that control law (10.73) ensures closed-loop stability in the presence of an arbitrary small time delay in the feedback loop only if $0 < k_{P\lambda} < 1$. Prove that this limitation does not hold for the integral gain of control law (10.74). [*Hint*: Use the first-order approximation $\lambda_{\text{env}}(t-\tau) \simeq \lambda_{\text{env}}(t) - \tau\dot{\lambda}_{\text{env}}(t)$ for the delayed force measurement on the right-hand side of (10.73) and (10.74), with delay $\tau > 0$.]

10.11 Compute the admittance of the controlled robot from the block diagram in Fig. 10.17 with $C_\nu(s)$ and $C_\lambda(s)$ as in (10.90) and analyse passivity. Analyze stability in the case of elastic environment, both with known and uncertain stiffness.

10.12 Compute the admittance of the controlled robot from the block diagram in Fig. 10.17 with $C_\nu(s)$ and $C_\lambda(s)$ as in (10.91) and analyse passivity. Analyze stability in the case of elastic environment, both with known and uncertain stiffness.

10.13 Compute the admittance of the controlled robot from the block diagram in Fig. 10.17 with $C_\nu(s)$ and $C_\lambda(s)$ as in (10.92), and using the modified force control (10.93). Analyze passivity. Analyze stability in the case of elastic environment, both with known and uncertain stiffness.